Title. An ST131 clade and a Phylogroup A clade bearing a novel *Escherichia coli* O-antigen cluster predominate among bloodstream *E. coli* isolates from southwest Nigeria hospitals.

Ayorinde O. Afolayan[1], Aaron O. Aboderin[2], Anderson O. Oaikhena[1], Erkison Ewomazino Odih[1], Veronica O. Ogunleye[3], Adeyemi T. Adeyemo[4], Abolaji T. Adeyemo[5], Oyeniyi S. Bejide[1], Anthony Underwood[6], Silvia Argimón[6], Monica Abrudan[6], Abiodun Egwuenu[7], Chikwe Ihekweazu[7], David M. Aanensen[6] and Iruka N. Okeke[1*].

[1]Global Health Research Unit for the Genomic Surveillance of Antimicrobial Resistance, Department of Pharmaceutical Microbiology, Faculty of Pharmacy, University of Ibadan, Oyo State, Nigeria.

[2]Department of Medical Microbiology and Parasitology, Obafemi Awolowo University Teaching Hospitals Complex, Ile-Ife, Osun State, Nigeria.

[3]Department of Medical Microbiology and Parasitology, University College Hospital, Ibadan, Oyo State, Nigeria.

[4]Department of Medical Microbiology and Parasitology, Obafemi Awolowo University Teaching Hospitals Complex, Ile-Ife, Osun State, Nigeria.

[5]Department of Medical Microbiology and Parasitology, University of Osun Teaching Hospital, Osogbo, Osun State, Nigeria.

[6]Centre for Genomic Pathogen Surveillance, Big Data Institute, University of Oxford, Old Road Campus, Oxford, United Kingdom and Wellcome Genome Campus, Hinxton, UK.

[7]Nigeria Centre for Disease Control, Jabi, Abuja, Nigeria.

***Corresponding author:** Iruka N. Okeke. Department of Pharmaceutical Microbiology, Faculty of Pharmacy, University of Ibadan, Oyo State, Nigeria. +234 805 328 1714. iruka.n.okeke@gmail.com

Abstract

Escherichia coli bloodstream infections are typically attributed to a limited number of lineages that carry virulence factors associated with invasion and, in recent years, invasive *E. coli* are increasingly multiply antimicrobial resistant. In Nigeria, *E. coli* is a common cause of bloodstream infections but the identity of circulating clones is largely unknown and surveillance of their antimicrobial resistance has been limited. We verified and whole genome-sequenced 68 bloodstream *E. coli* isolates recovered between 2016 and 2018 at three sentinel sites in southwestern Nigeria and susceptibility tested 67 of them. Resistance to antimicrobials commonly used in Nigeria was high, with 67(100%), 62 (92.5%), 53 (79%) and 37(55%) showing resistance to trimethoprim, ampicillin, ciprofloxacin and aminoglycosides, respectively. All the isolates were susceptible to carbapenems and colistin. The strain set included isolates from globally disseminated high risk clones including those belonging to ST12 (n=2), ST131 (n=12) and ST648 (n = 4). Twenty-three (33.82%) of the isolates clustered within two clades. The first of these consisted of ST131 strains, comprised of O16:H5 and O25:H4 sub-lineages. The second was an ST10-ST167 complex clade comprised of strains carrying capsular genes that may have originated in *Klebsiella*. We additionally determined that four temporally-associated ST90 strains from one sentinel were closely related enough to suggest that at least some of them represented a retrospectively detected outbreak cluster. Our data demonstrate that a broad repertoire of invasive *E. coli* isolates cause bloodstream infections in southwest Nigeria. In addition to pandemic lineages, particularly ST131, these include a previously undescribed lineage carrying an O-antigen cluster previously only reported from *Klebsiella*. Genomic surveillance is valuable for tracking these and other clones and for outbreak identification.

Keywords: *Escherichia coli*, Genomic Surveillance, ST131, antimicrobial resistance, *cpsACP*, Nigeria

Data Summary

Phylogenetic tree, clinical data, and epidemiological data were visualized using Microreact (https://microreact.org/project/hmj3KwxS1dmmFPCKFx6qeA-invasive-escherichia-coli-sw-nigeria-2016-2018). All the sequence data have been deposited in the ENA under the project ID PRJEB29739 (https://www.ebi.ac.uk/ena/browser/view/PRJEB29739). Accessions can be found in Table S6.

Introduction

Extra-intestinal pathogenic *Escherichia coli* (ExPEC) are responsible for the majority of infections in the blood, urine, meninges, prostate, and other normally sterile sites [1–3]. Although typically initially acquired within the gastrointestinal tract (and less commonly via genital route), these strains of *E. coli* differ from commensal and diarrhoegenic *E. coli* in possession of factors associated with systemic virulence [4, 5], allowing them to survive in different extra-intestinal niches. Some of the virulence genes associated with ExPEC include adhesins (*fim*, *pap*, *sfa*, *afa*), invasins (*ibeA*), iron acquisition genes (*ybt*, *iro*, *iuc*), toxins (*clb*, *cnf*, *hly*, SPATE genes) and protectins (*traT*, *ompT*, *kpsMT*), among others [4, 5]. ExPEC also often have K, O and H antigens that make them recognizable to *E. coli* experts and, in some instances, assist them in evading immune responses. Virulence and AMR determinants, as well as negative frequency-dependent selection, likely influence the stability of the most dominant ExPEC groups, which are often multiply resistant [6], thereby sustaining the occurrence of extra-intestinal diseases globally. In Africa, available data reveal that there is an upward trend in the prevalence of globally dominant ExPEC lineages in humans [7] and animals [8], painting a grim picture for disease and antimicrobial resistance.

Robust surveillance is urgently needed to tackle antimicrobial resistance in a more robust and consistent manner within each country. Whole genome sequencing (WGS) has helped to provide a clearer picture on the epidemiology of infectious diseases caused by ExPEC and has identified a number of pandemic clones. Incorporation of WGS with existing epidemiological frameworks in national public health institutes is critical for providing genomic context for prospective surveillance and for designing and implementing AMR-eliminating strategies.

Although studies conducted in Africa and other low- and middle-income countries (LMICs) have shown the abundance of invasive *E. coli* [9, 10], these studies are too few and far between so that ExPEC and AMR epidemiology are poorly understood [7, 11]. In Nigeria, there is sparse molecular information on ExPEC, but a few studies point to likely clonal expansion of resistant lineages and local presence of pandemic clones of concern [12–16]. These studies provide valuable information but represent an insufficient picture of ExPEC clones in Nigeria with few data available from the South. To extend the body of knowledge on genomic epidemiology of ExPEC in south western Nigeria, including AMR patterns and mechanisms, we leveraged on our

existing genomic surveillance of bacterial AMR efforts by characterizing the genomes of invasive isolates from tertiary hospitals in South-west Nigeria.

Methodology

Species Validation and Antimicrobial Susceptibility Tests

Sentinel hospital laboratories referred anonymized clinical data and bloodstream *E. coli* isolates collected between the years 2016 to 2018 to the National Reference Laboratory for verification of isolate identity and antimicrobial susceptibility tests (AST). Isolate identity and AST were achieved using the VITEK2 Instrument. Drugs tested include amikacin (AMK), gentamicin (GEN), ampicillin (AMP), amoxicillin/clavulanic acid (AMC), piperacillin/tazobactam (TZP), cefuroxime (CXM), cefuroxime axetil (CXMA), cefepime (FEP), ceftriaxone (CRO), cefoperazone/sulbactam (SFP), nitrofurantoin (NIT), nalidixic acid (NAL), ciprofloxacin (CIP), ertapenem (ERT), imipenem (IPM), meropenem (MEM), and trimethoprim-sulfamethoxazole (SXT). Resistance profiles were generated from VITEK2 AST data. Antibiotic susceptibility results were interpreted in line with the CLSI 2019 standards [17]. Minimum Inhibitory Concentration values were converted to RIS values and the bug-drug combination table was generated using the AMR R package (v1.4.0; https://github.com/msberends/AMR) [18].

Biofilm Assay

Following Wakimoto's procedure [19], we sub-cultured invasive *E. coli* strains overnight in LB broth at 37°C with shaking at 160 rpm. Afterwards, we measured 190 µL of Dulbecco's Modified Eagle's Medium (DMEM) containing 0.45 % glucose using a pipette into each well of a 96-well plate (different plates were used for each time point (3h, 6h, 12h, 24 h)). Five µL of each isolate was inoculated in triplicate per time point into a 96-well plate from the stock plate and incubated at 37°C without shaking until each time point was reached. Absorbance at 595 nm was taken on completion of time point.

We pipetted spent media out of the 96-well plates. Each well was washed with PBS three times, fixed (10 mins, 200 µL of 75% ethanol), dried, and stained with 195 µL of 0.5 % crystal violet

for 5 minutes. This was followed by washing and drying of the plates. We added 200 µL of 95% ethanol to each well, allowed the wells to stand for 20 minutes at room temperature, and determined absorbance with an enzyme linked immunosorbent assay (ELISA) plate reader at 570 nm. Biofilm index was defined using the average of the values for the optical density (OD) at 570 nm and 595 nm, and was calculated by dividing the OD values for each strain at a given timepoint by the OD values of the negative control at the given timepoint [20]. Enteroaggregative *E. coli* strain 042 was used as positive control while *E. coli* K-12 DH5α was used as negative control. The magnitude of biofilm formed by different genetically defined subgroups of isolates was compared using a two-tailed Mann-Whitney test at $p<0.05$.

Haemolysis Test

Overnight LB cultures of the isolates were spotted onto the surface of the blood agar. Alpha haemolysis and beta haemolysis is indicated by a green colouration and a clear zone around bacteria colonies, respectively. Uropathogenic *E. coli* isolate ATCC 11175 and *stx*-deleted *E. coli* O157 isolate ATCC 7000728 were used as controls.

DNA Extraction, Library Preparation, and Whole Genome Sequencing

Genomic DNA was extracted following the protocol outlined in a previous report [21]. Briefly, the Wizard DNA extraction kit (Promega; Wisconsin, USA; Cat. No: A1125) was used in the extraction of genomic DNA of all isolates. A dsDNA Broad Range quantification assay was used in the quantification of DNA extracts (Invitrogen; California, USA; Cat. No: Q32853). DNA libraries were prepared and sequenced using the NEBNext Ultra II FS DNA library kit (New England Biolabs, Massachusetts, USA; Cat. No: E6617L) and Illumina HiSeq X10 instrument (Illumina, CA, USA), respectively.

Genome Assembly and Speciation

Raw sequence reads were assembled using the GHRU pipeline (https://gitlab.com/cgps/ghru/pipelines/assembly) which is summarily explained by the GHRU

de novo assembly protocol [22] . Speciation was possible using Bactinspector (v0.1.3; https://gitlab.com/antunderwood/bactinspector/), implemented within the GHRU pipeline.

Single Nucleotide Polymorphism (SNP) Analysis and Phylogenetic Tree Generation

The complete chromosome sequence of *Escherichia coli* strain EC958 (accession GCF_000285655.3) (https://www.ncbi.nlm.nih.gov/assembly/GCF_000285655.3/) was used to infer a whole-genome alignment of the sequence reads and identify SNP positions, which were, in turn used to infer a maximum-likelihood phylogenetic tree as per the GHRU mapping-based phylogeny protocol [22] which summarizes the steps implemented within the GHRU SNP phylogeny pipeline (https://gitlab.com/cgps/ghru/pipelines/snp_phylogeny).

Isolates that clustered closely within the phylogenetic tree, belonged to the same ST, and shared similar resistance profiles, plasmid profiles, geography and dates of isolation, were investigated further for clue on potential outbreaks. We selected the closest reference genome to the outbreak isolates using Bactinspector, aligned the outbreak isolates (ST90) to the reference genome of *E. coli* strain D3 (accession NZ_CP010140.1; https://www.ncbi.nlm.nih.gov/assembly/GCF_001900635.1/), used Gubbins [23] to mask recombinant regions, and calculated pairwise SNP distances from the pseudo-genome alignment using FastaDist (v0.0.7; https://gitlab.com/antunderwood/fastadist), SNP-dists (v0.8.2; https://github.com/tseemann/snp-dists), and/or the R package harrietr (v0.2.4; https://github.com/andersgs/harrietr). The adegenet R package (v2.1.5; https://github.com/thibautjombart/adegenet/) was used to generate a pseudogenome alignment in DNA.bin format (one of the input files accepted by harrietr) from a pseudogenome alignment file. Phylogenetic tree, epidemiological data and in silico data were visualized in the web-based viewers Microreact [24], and the interactive Tree Of Life (iTOL) [25].

AMR gene, Virulence gene, and Plasmid Replicon Prediction

The program SRST2 (v0.2.0; https://github.com/katholt/srst2/) [26] and the ARGannot database (https://raw.githubusercontent.com/katholt/srst2/master/data/ARGannot_r3.fasta) were used to screen raw sequence reads for the presence of acquired resistance genes. We also validated the

report/output by utilizing the GHRU AMR Pipeline (https://gitlab.com/cgps/ghru/pipelines/dsl2/pipelines/amr_prediction) as explained in this protocol [22]. *ampC1* and *ampC2* were excluded from downstream analysis and visualization as they are beta-lactamase genes present in almost all *E. coli* isolates and are unlikely to confer antibiotic resistance in *E. coli* [27]. Overall plot of resistance determinants was constructed using the *upset* function from the UpSetR package (v1.4.0) [28]. Plots of AMR genes stratified by sequence type and sentinel site were constructed using the ggupset package (v0.3.0). Association between virulence genes and phylogroups of *E. coli* was determined using the *fisher_test* function from the rstatix package (v0.7.0). The calculation is based on single genes (including those that make up an operon), not operons. The associations were corrected for multiple testing using the Bonferroni method offered by rstatix. Bar plots were visualized using the *ggplot* function from the Tidyverse package (v1.3.1) in R.

The raw reads were screened for virulence genes with the GHRU pipeline, which utilizes ARIBA [29] and the VFDB database [30]. Plasmid replicon types were determined with same GHRU pipeline but using the PlasmidFinder database instead [31].

Multilocus Sequence Typing (MLST) profiling

Following the Achtman MLST scheme [32], multi-locus sequence types (STs) were determined using the SRST2 program. We confirmed the results by using the GHRU MLST pipeline, which also implements the Achtman scheme. as summarized in the aforementioned GHRU protocol [22].

***In silico* Serotyping and Phylogroup Determination**

The O and H serotypes of *Escherichia coli* were determined using the SRST2 program and the EcOH database (https://raw.githubusercontent.com/katholt/srst2/master/data/EcOH.fasta). This result was validated using ECTyper (v1.0.0; https://github.com/phac-nml/ecoli_serotyping) and SerotypeFinder (https://bitbucket.org/genomicepidemiology/serotypefinder/src/master/). SerotypeFinder utilizes KMA [33] and BLAST+ [34] to predict *E. coli* serotypes from the

alignment of raw and assembled reads, respectively, against the SerotypeFinder database. *Escherichia coli* genomes were assigned into phylogroups using ClermonTyping (v20.03) [35].

Concordance

The agreement between phenotypic and genotypic antimicrobial resistance was determined for beta-lactams, cephalosporins, amikacin/kanamycin/gentamicin, trimethoprim, and the quinolones. Metrics such as sensitivity, specificity, true positives, true negatives, false positives, and false negatives were determined using the R script (https://gitlab.com/-/snippets/2050300, first used in a previous report) which utilizes the *epi.tests* function within the epiR package (v2.0.26) for each antimicrobial tested. Here, "Sensitive" and "Intermediate" values were combined, taking cognizance of the arguments for and against the use of the term "Intermediate" in clinical settings [36].

Genome Annotation, Comparative Genomics, and gene location prediction.

Functional annotation of Onovel32 clade genomes was performed using Bakta v1.0.4 [37] . Genomes were compared and visualized using Artemis v18.1.0 [38], Artemis Comparison Tool v18.1.0 [39], and Clinker v0.0.21 [40]. The mlplasmid web tool [41] was used to predict whether clinically-relevant virulence genes were borne on plasmids or on chromosomes.

Results

Epidemiology and Species Identification

Three hospital laboratories in South-west Nigeria submitted retrospective bloodstream *Escherichia coli* isolates with clinical and epidemiological data between the years 2016 to 2018. Available data showed that isolates were collected from patients aged 1 day to 71 years, with 17 (25%) of the isolates recovered from children under 60 days old (range 1- 20 days, median 9 days), who would be characterized as neonates. The isolates were submitted from the University College Hospital (UCH; n = 22), Obafemi Awolowo University (OAU) Teaching Hospitals

Complex (n = 18), and Osun State University Teaching Hospital, Teaching Hospital (until recently known as Ladoke Akintola University) (LAU; n = 28).

Of the 68 invasive isolates confirmed as *E. coli* by whole-genome sequencing (WGS), 48 (70.6%) and 64 (94.1%) were correctly identified as *E. coli* by the sentinel biochemical testing and reference laboratory VITEK2, respectively. *Escherichia coli* isolates were often misidentified as *Klebsiella pneumoniae* (n = 8) or *Citrobacter freundii* (n = 6) at the sentinel laboratories, while the VITEK2 system misidentified *E. coli* as *Klebsiella pneumoniae* (n = 3) or *Enterobacter aerogenes* (n = 1).

Phylogroups, serotypes, and sequence types of *E. coli* bloodstream isolates

E. coli sent from all three hospital sentinel laboratories spanned all *E. coli* phylogroups, with 18, 15, 19, 8, 2, 1, and 5 *E. coli* genomes classified within phylogroups A, B1, B2, C, D, E, and F, respectively. The most common STs among the 33 identified include; ST131 (n = 12), ST156 (n = 5), and 4 each of ST10, ST167 ST410, ST648, and ST90. These 7 STs accounted for 54% of the *E. coli* isolates. Of these, only STs 131 and 167 were found across the 3 sentinel sites (Figure 1, Table S4). Diverse lineages were recovered from all three sentinel sites (OAU = 10 STs; LAU = 18 STs, UCH = 15 STs) (Table 1). While ST131 genomes made up 63% of genomes within phylogroup B2 (the second most common phylogroup), ST10 and ST167 genomes accounted for 44% of genomes within phylogroup A (the most common phylogroup).

While none of the isolates were submitted as suspected outbreak strains, , four isolates recovered from LAU within one month (January 2017) were typed as ST90, serotype O8:H9, carried the same plasmid profile (IncFI; IncFIA; IncFIB_AP001918; IncQ1), AMR gene profile, and similar but not identical resistance profile (Table S4). These four isolates were resistant to trimethoprim, the quinolones, gentamicin, cefuroxime axetil, and ampicillin (Table S3b). Comparison of pairwise SNP differences revealed that two of the four isolates were identical while the other two isolates differed from these by 11 SNPs and 72 SNPs. The current literature supports a clustering threshold between the range of 0 to 17 SNPs for suspected outbreak-related *E. coli* blood isolates [42–44]. Although these isolates were correctly identified within this sentinel site, the cluster was only recognized retrospectively, likely due to different beta lactam resistance profiles.

ST131 was the most common sequence type detected and the 12 isolates belonging to this ST clustered into two distinct lineages defined by serotype H5 (n = 5; O16:H5) and the serotype H4 lineage (n = 7; O25:H4), and henceforth referred to as the ST131 lineage 1 and ST131 lineage 2, respectively (Figure 1).

A total of 38 unique serotypes and 25 O-groups were identified. Of note was the most common O-type, which was novel and identified in eleven isolates belonging to phylogroup A. These ONovel:32 strains belonged to ST10 or ST167, or were single or double locus variants of these STs. They included six ONovel32:H10 isolates as well as three H21 and one H4 –flagellin-encoding strains. Along with one ONT:H10 strain that also belonged to ST10, they formed a distinct clade on the phylogenetic tree (Figure 1). Strains belonging to this cluster were submitted from all three hospitals. Two of them were originally misclassified as *Klebsiella pneumoniae* by VITEK2 at the reference laboratory level. Irrespective of whether the ST90 clade is discounted, the ONovel:32 clade and the ST131 clade were the most abundant. Together they accounted for 32.4 % of the isolates and both clades were found in all three hospitals (Figure 1).

Virulence Factor Profiles of the Bloodstream *E. coli* Isolates

Diverse virulence genes were observed among the ExPEC genomes: 159 virulence-associated (VAG) genes were found at least once in the 68 bloodstream isolate genomes. Enterobactin genes (*entB*, *entC*, *entE_1*, *entS*) and ferrienterobactin precursors and proteins (*fep* operon genes (ABCDEG) and *fes_1*), were found in more than 95% of the isolates. The outer membrane hemin receptor (*chu*), siderophores (*fyuA*, *irp*, *ybt*), intimin-like adhesin (*fdeC*), haemolysin (*hly*), aerobactin (*iuc*), polysialic acid transport protein *kpsM_1*, pyelonephritis-associated pili *pap*, SPATE genes (*sat*, *vat*), and plasmid-encoded *Shigella* enterotoxin *senB* were more abundant and significantly more associated with phylogroup B2 than with phylogroups A, B1, and C (Fisher's exact Test, $p < 0.05$; Figure 2a). Figure 2b shows that a wide range of biofilm-forming capacities were seen in the subset of isolates tested with moderate or strong biofilm-formers being most common in phylogroups B1 and B2 as well as the ST90 outbreak strain-containing

phylogroup C. No significant difference in biofilm-formation between the phylogroups was observed.

Phylogroup B2 isolates, comprised largely of ST131 strains, carried the highest number of virulence-associated genes (n = 86 VAGs). Thirty-four VAGs were significantly more common in ST131 isolates (n = 12) than in non-ST131 isolates (n = 56). Of these the genes encoding the outer membrane haem receptor (*chu*), yersiniabactin (*ybt*), and pyelonephritis-associated pili (*pap*) were found in more than 84% of the ST131 isolates (Fisher's exact Test, $p < 0.05$; Fig. 3a). On the other hand, 6 VAGs were significantly more common in non-ST131 isolates than in ST131 isolates, including 2 genes (*gspK* and *gspL*) present in more than 85% of the non-ST131 isolates, but in only about 50% of ST131 isolates. The VAGs *entD*, *espL1* , *espX1*, and *espL5* were absent in ST131 isolates but were present in at least 32% of non-ST131 isolates, notably Phylogroup A ONovel32 strains (Fig. 3a).

Both lineages of ST131 share common VAGs, including; adhesins, yersiniabactin, aerobactin, enterotoxin, and transport-associated genes but some genes were only seen, or predominantly seen in one of the two lineages. For example, the haemolysin (*hly*) carried by two isolates within ST131 lineage 2 were absent in ST131 lineage 1. Also, two isolates within ST131 lineage 2 carried the cytotoxic necrotizing factor *cnf1*. (Figure 3a and 3b). The median pairwise distance between isolates in ST131 lineage 1 is 2857.5 SNPs (range: 0 – 2866), while the median pairwise distance between isolates within ST131 lineage 2 is 499 SNPs (range: 0 – 827). The inter-clade SNP distance is 13619 (range: 12900 – 14146) (Figure S1).

None of the ONovel32 clade isolates carried alpha haemolysin or pyelonephritis associated pili, which were present in ST131 and some of the other lineages. However, some virulence-associated genes were predominant among or restricted to ONovel32 strains (Figure 4a and 4b). These include the *esp4L* type III secretion effector. We also searched independently for type III secretion systems and identified a cluster 97.5% identical to *E. coli* type III secretion system 2, previously associated with virulence in septicemic *E. coli* [45], in all *esp4L*-positive and one *esp4L*-negative Onovel32 isolate (GI8584164). *esp4L* was more common among these isolates than other phylogroup A strains as well as multiple genes encoding capsular modification

enzymes. All the ONovel32 strains and one associated ONT strain carried a *ugd* gene. The only other isolates in this collection with this gene were three isolates belonging to the globally disseminated high risk clone ST648 [46], known to possess biofilm-associated features that enhance pathogen emergence and persistence in both the human body and the environment. The *ugd* gene is associated with hypermucoviscosity and invasive virulence and the ONovel32 allele is 96% identical to that from *K. pneumoniae* NTUH-K2044, a hypervirulent *K. pneumoniae* isolate [47] and *K. variicola* (Accession number CP079802.1) capsular cluster *ugd* genes. Six of the ONovel:32 strains (but not the ONT:H10 strain in the same clade) carried *cpsACP*, a chromosomally-borne gene, which is predicted to encode a phosphatidic acid phosphatase (PAP2 Pfam 01569) family gene. PAP2 phosphatases replace phosphate groups on lipid A with amine groups resulting in a positively charged lipid A that confers resistance to cationic peptides [48]. PAP2 phosphatases have been known to be transmitted horizontally solitarily or as part of capsular clusters [49]. A BLAST search revealed that the ONovel32 PAP2 allele is 99.6% identical to endogenous PAP2 genes from *Klebsiella variicola* (Accession number CP079802.1). As shown in Figure 5, depicting the region for ONovel32 ST1284 strain OAU-VOA-056, *cpsACP* is located within a capsular gene cluster identical to a *K. variicola* cluster and flanked by a 5' IS3 transposase and a 3' IS1 protein InsB-encoding gene. At the opposite end of the cluster is the *ugd* gene. The cluster shows G+C content and other base-pattern signatures that depart from the *E. coli* flanking sequence (Figure 5a and 5b).

Observing that ONovel:32 cluster isolates, some of which were originally misclassified as *Klebsiella*, showed mucoidity upon plate culture, we sought to determine whether these strains had distinctive colonization-associated capacities. The median A_{570} at six hours was 0.178 for phylogroup A strains lacking *cpsACP* and 0.216 for those with the gene (Figure 2), but these differences were not significant. All the isolates were also negative in the string test for hypermucoviscosity in *Klebsiella* [50].

Resistance Profiles (RP) and Concordance with Predicted Antimicrobial Resistance

Susceptibility testing of 67 out of the 68 isolates showed that, of the 16 antibiotics tested, resistance to trimethoprim-sulfamethoxazole (n = 67; 100%), ampicillin (n = 62; 92.5%), nalidixic acid (n = 57; 85.1%), and ciprofloxacin (n = 53; 79.1%) was commonly observed (Fig. 6a, Fig. 6b, Table S2). On the other hand, resistance to cefoperazone.sulbactam (n = 3; 4.5%) was less common. All isolates were susceptible to amikacin, ertapenem, , and meropenem (Table S2, Fig. S1a and S1b). One $bla_{CTX\text{-}M\text{-}15}$ –positive isolate from LAU (ST11025, B1, O51:H12) was categorized as showing intermediate to imipenem but did not carry any carbapenemase-producing gene. Resistance profiles were remarkably similar among the three sentinels (Figure 6b). Resistance to trimethoprim/sulfamethoxazole among isolates belonging to all 33 STs could be explained by the possession of *dfrA* (n = 54/67) and *dfrB* (n = 2/67) genes. Ciprofloxacin resistance (23 STs) was largely attributable to mutation in the quinolone resistance determining regions (QRDR) of *gyrA* (D87N, S83L), *parC* (E84A, E84G, E84K, S57T, S80I), and/or *parE* (E460D, I355T, I529L, I529L, I464F, L416F, L445H, S458A, S458T), with or without the presence of plasmid quinolone resistance genes (*qnrS*, *qnrVC4*, *qepA*, *aac-(6')-Ib-cr*). About 45% (n = 24/53) of isolates phenotypically resistant to ciprofloxacin carried a combination of *aac(6')-lb-cr5* gene and mutation in the QRDR regions (*gyrA*, *parC*, and *parE*) (Figure 7a and 7b). The most common quinolone resistance gene profile observed is the "gyrA_D87N,gyrA_S83L,parC_S80I,parE_S458A", as observed in a quarter (n = 14/53) of isolates showing phenotypic resistance to ciprofloxacin.

Ampicillin resistance among isolates belonging to 29 STs (n = 62) could be explained by the carriage of a range of beta-lactamase genes including $bla_{TEM\text{-}1}$ (36/62 of isolates), $bla_{TEM\text{-}40}$ (3 isolates), $bla_{TEM\text{-}84}$ (2 isolates), $bla_{TEM\text{-}135}$ (2 isolates), , or $bla_{OXA\text{-}2}$ (co-occurring with $bla_{TEM\text{-}90}$; 1 isolate). Extended-spectrum beta-lactam resistance likely resulted from $bla_{CTX\text{-}M\text{-}15}$, $bla_{CTX\text{-}M\text{-}27}$, and $bla_{CMY\text{-}42}$ (Figure S2a and S2b) co-occurring largely with the plasmids Inc types FIB_AP001918, FIA, IncFI, IncQ1, IncFII_p, and the col plasmid Col156.

Of the 5 drug classes tested, the highest concordance between phenotypic resistance and predicted antimicrobial resistance was observed for trimethoprim (100% concordance, TP = 67/67, Sensitivity = 100%, Specificity = NA) and the lowest concordance for drugs within the

aminoglycoside class (concordance = 55.22%, TP = 37/67, Sensitivity = 100%, Specificity = 0 %) (Table S3a).

Multidrug Resistance (MDR)

We observed a total of 23 resistance profiles (RP) (Table S1) with resistance profiles in many cases associated with specific STs (Table 1 and Table S4). Fifty-nine (88.06%) of the isolates were resistant to at least one agent within at least three classes of antibiotics, fitting the multi-drug resistant (MDR) definition of the international AMR community [51] (Table S1). Isolates belonging to the most frequent sequence types form the bulk of invasive isolates carrying ESBL genes or mutations in the quinolone-resistance determining regions (*gyrA*, *parC*, *parE*), and the plasmid-mediated quinolone resistance gene *aac(6')-lb-cr*, as well as genes conferring resistance to trimethoprim. Carbapenemase genes were conspicuously absent, in agreement with the AMR phenotype. Almost all isolates carrying ESBL genes (n = 32/34) are multidrug resistant. About 30% of these showed the most frequent resistance profile (RP-1) (Figure S3). Furthermore, multi-drug resistant bloodstream isolates do not carry the same resistance determinants and plasmid replicons, apart from *gyrA/parC/parE* mutations (Figure S3).

Resistance gene profiles differed significantly between the two ST131 clades (Figure 3c). Unlike ST131 lineage 1 isolates, ST131 lineage 2 isolates did not carry any beta-lactamase gene besides *ampC*. Within the ST131 lineage 1, two isolates did not carry genes conferring resistance/reduced susceptibility to the aminoglycosides, phenicols, macrolides, and quaternary ammonium compounds. Furthermore, the absence of the Col156, IncB_O_K_Z, and IncFI plasmids in these two isolates seem to have been compensated by the possession of IncFIA, IncFII_p, and IncI1 plasmids, noted to have been absent in the other three ST131 isolates within the ST131 lineage 1.

All the ONovel32 strains (but not the co-clustering ONT strain) carried one ESBL gene, $bla_{CTX\text{-}M\text{-}15}$, and these strains also carried IncF plasmids, common among phylogroup A strains (Table S4, Table S5). Every one of them carried the most common four resistance-conferring mutations in

the QRDRs (gyrA_D87N,gyrA_S83L,parC_S80I,parE_S458A) and seven, including the ONT strain, carried *qepA4*. Four ONovel32 isolates additionally carried *aac-(6')-Ib-cr*, conferring aminoglycoside and ciprofloxacin resistance, as well as horizontally-transmitted genes conferring resistance to trimethoprim, chloramphenicol and tetracyclines were common (Microreact link, Table S5).

Common to both the ST131 and the ONovel:32 clades is the high prevalence of *qacEdelta1* (n = 9 and 8, respectively) conferring resistance to quaternary ammonium compounds, commonly used for disinfecting hospital surfaces and associated with class 1 integrons. Altogether, these clades comprised 17 (42.50%) of 40 *E. coli* isolates carrying this gene.

Discussion

This study characterized 68 bloodstream *E. coli* isolates as an important first step in understanding their epidemiology within south-west Nigeria. In this small collection, we identified multiple clones of pandemic importance, and found two predominant clades. One of these, comprised of two ST131 lineages is globally disseminated and this study illustrates its importance in Nigerian health facilities. The second predominant clade does not feature in present discourse on international ExPEC clones and represents strains belonging to ST10, ST167 and related STs, which predominantly encode genes that could confer a novel O-antigen type. In addition to these prominent clades, we identified strains belonging to major pandemic ExPEC lineages, including ST12, ST73, and ST648, and their single locus variants. ST69, ST95, and ST405 lineages were not detected but our sample is not very large and therefore our findings are insufficient to rule them epidemiologically insignificant in our setting. We additionally identified in the collection five ST90/410 strains, all from a single facility. Two ST90 isolates are identical, differ from a third by only 11 SNPs, and likely represent an outbreak. Our findings add to information that is chronicling ExPEC lineages of importance within Nigeria [14–16, 52, 53], other parts of Africa [16, 54], and other low- middle-income countries [16, 55].

Among ST131, we found both globally-disseminated lineages within our isolate collection. The majority of haemolytic and *pap* gene-bearing phylogroup B2 strains belonged to this ST. Biofilm formation among these strains was common and associated with the *kpsD* gene, a known contributor to biofilm formation [56]. The ST10, ST167 and related strains that comprised the ONovel32 clade were distinguished by the presence of one of two variations of a capsular island that has been well described in *Klebsiella* with biofilm formation among them being more pronounced among strains carrying the *cpsACP*-containing portion of the island. While the virulence of ST131 has been well described, features of this clade that cause it to predominate remain unknown and further studies are required to understand its pathogenicity and selective success in our setting.

High levels of phenotypic resistance to antibiotics within the antifolate (trimethoprim. co-trimoxazole), quinolone (nalidixic acid), fluoroquinolone (ciprofloxacin), cephalosporin (cefuroxime axetil), and the aminoglycosides (gentamicin) classes observed among invasive isolates in this study corroborates reports from previous studies [12, 52, 53] and pose a serious concern for clinical therapeutics. *In silico* data confirm the abundance of genes conferring resistance, with many isolates carrying more than one gene conferring resistance to a specific antimicrobial or class. Before the turn of the millennium, resistance to many of the aforementioned antimicrobials was rare in Africa. However, steady increase in the availability and use of these agents in the empiric treatment of ExPEC-related infections has inevitably selected for AMR. The increased rate of fluoroquinolone resistance in diarrhoeagenic *E. coli* and other enterobacterales, for instance, coincided with increased fluoroquinolones use in Nigeria [57] and other parts of Africa [7, 58]. While findings from a study conducted in Nigeria more than a decade ago [13] concluded that nalidixic acid was still an effective antimicrobial, we observed in this study that resistance to nalidixic acid is now common.

Similarly, cephalosporin resistance emerged and expanded much more in Africa than in other parts of the world as these agents became the drug of choice for treating multi-drug resistant pathogens [58]. Fluoroquinolone resistance has also been previously associated with the presence of ESBL genes because ESBL genes are often borne on transferable large plasmids that co-host some of the PMQR genes [59]. We observed the co-carriage of ESBL and fluoroquinolone

resistance genes in more than a quarter of the ExPEC isolates, and particularly in over-represented lineages.

We find that both predominant lineages we have highlighted in this report show multiple resistance. This has important implications for patients with life-threatening bloodstream infections and provides a plausible explanation for their evolutionary success in our setting. Resistance to antimicrobials used intensively in Nigeria (trimethoprim, aminopenicillins and ciprofloxacin) was rife and resistance to the agents most frequently used empirically when blood stream infections are suspected – second- and third-generation cephalosporins and aminoglycosides was also worryingly common. While none of these clades showed carbapenem or colistin resistance, these reserve antimicrobial classes are out of the reach of most patients attending the three hospitals from which the strains were obtained.

Next-generation sequencing has emerged as a promising complement to clinical bacteriology as it provides answers to medical conundrums as well as a more robust picture of the epidemiology of infectious diseases. It can also reveal, as in this case, circulation of hitherto unrecognized clones of concern. Although its integration into clinical diagnosis and patient care gaining ground many parts of the world, its adoption in LMICs (and the rest of the globe) is still hindered by lack of infrastructure, cost of implementing WGS, limited bioinformatics expertise and as yet mildly inaccurate prediction of antimicrobial resistance [60, 61]. In our study, we observed perfect concordance (100%) with phenotypic AST data for trimethoprim, but not for the cephalosporins, the quinolones, or the aminoglycosides. This therefore shows that further understanding of resistance mechanisms and routine AMR database update is needed to enhance the feasibility of gradual and sustained integration of WGS into routine diagnosis.

Another advantage of next-generation sequencing is its potential in rapid detection of outbreaks either retrospectively, or in real-time. We report a likely retrospective ST90 outbreak in LAU, which would not have been detected using traditional diagnostic methods in the sentinel laboratories. ST90 strains have variously been highlighted for their zoonotic potential and association with device-related hospital outbreaks [62–64] and its epidemiology in our setting remains to be understood ST90, and related ST410, were only seen at one facility and the representation of ST90 at this facility may have been amplified by an outbreak. The adoption of

genomic surveillance in diagnostic laboratories within Nigeria will ensure that outbreaks of this and other clones can be detected in real time, while definite tracking and containment of the spread of such clones will be achieved before lives are lost.

This study has a few limitations. Blood culture is infrequently performed in Nigerian hospitals and until recently, most isolates were not archived. Therefore, these isolates represent but a fraction of the ExPEC likely to have infected patients in the three hospitals and may not be representative. Our short-read data makes it impossible to accurately determine whether the resistance genes are located on the bacterial chromosome or plasmids (or other mobile genetic elements). In future, we will incorporate long read sequencing into our prospective surveillance efforts in order to correctly identify plasmid-borne AMR genes.

In conclusion, this study provided hospital-specific information on the population structure of ExPEC lineages needed to track pandemic lineages and guide infection disease control practices in line with Nigeria's national action plan on antimicrobial resistance.

Author Statements

Conceptualization: David M. Aanensen, Iruka N. Okeke, Chikwe Ihekweazu; **Data curation**: Ayorinde O. Afolayan, Anthony Underwood; **Formal Analysis**: Ayorinde O. Afolayan, Anthony Underwood, Oyeniyi S. Bejide, Iruka N. Okeke; **Funding acquisition**: David M. Aanensen, Aaron O. Aboderin, Iruka N. Okeke; **Investigation**: Ayorinde O. Afolayan, Abiodun Egwuenu, Erkison Ewomazino Odih, Oyeniyi S. Bejide, Aaron O. Aboderin, Iruka N. Okeke; **Methodology**: Ayorinde O. Afolayan, Aaron O. Aboderin, Anderson O. Oaikhena, Erkison Ewomazino Odih, Oyeniyi S. Bejide, Veronica O. Ogunleye, Adeyemi T. Adeyemo, Abolaji T. Adeyemo, Anthony Underwood, Silvia Argimón, Monica Abrudan, David M. Aanensen, Iruka N. Okeke; **Project administration**: Abiodun Egwuenu, Chikwe Ihekweazu, Aaron O. Aboderin, Iruka N. Okeke; **Resources:** Anthony Underwood, Silvia Argimón, Veronica O. Ogunleye, Adeyemi T. Adeyemo, Abolaji T. Adeyemo, David M. Aanensen, Iruka N. Okeke; **Software:** Ayorinde O. Afolayan, Silvia Argimón, Anthony Underwood; **Supervision:** Aaron O. Aboderin, Anthony Underwood, Silvia Argimón, Chikwe Ihekweazu, David M. Aanensen, Iruka N. Okeke; **Validation:** All authors; **Visualization:** Ayorinde O. Afolayan, Iruka N. Okeke; **Writing – original draft:** Ayorinde O. Afolayan; **Writing – review & editing:** All authors.

Acknowledgments/Funding

We thank Damilola Q. Olaoye, Chinenye Ekemezie, Ifeoluwa Akintayo and Ifeoluwa Komolafe for excellent technical assistance.

This work was supported by Official Development Assistance (ODA) funding from the National Institute of Health Research [grant number 16_136_111] and the Wellcome Trust grant number 206194. INO was an African Research Leader supported by the UK Medical Research Council (MRC) and the UK Department for International Development (DFID) under the MRC/DFID Concordat agreement that is also part of the EDCTP2 program supported by the European Union. The funders had no role in the content, crafting or submission of this paper.

Ethics

Isolates were obtained as part of the surveillance efforts in line with Nigeria's national action plan and/or for bloodstream pathogen and *Escherichia coli* research. In Nigeria. Ethical approval for research using these isolates was obtained from the University of Ibadan/University College Hospital and the Obafemi Awolowo University (OAU) Teaching Hospitals complex ethics commitees. Respective IRB registration numbers are UI/EC/15/093 and ERC/2017/05/06.

Conflicts of Interest

The authors have no conflicts of interest to declare.

References

1. **de Kraker MEA, Jarlier V, Monen JCM, Heuer OE, van de Sande N, *et al.*** The changing epidemiology of bacteraemias in Europe: Trends from the European antimicrobial resistance surveillance system. *Clin Microbiol Infect* 2013;19:860–868.

2. **Foxman B**. The epidemiology of urinary tract infection. *Nature Reviews Urology* 2010;7:653–660.

3. **Manges AR, Geum HM, Guo A, Edens TJ, Fibke CD, *et al.*** Global extraintestinal

pathogenic escherichia coli (Expec) lineages. *Clin Microbiol Rev*;32. Epub ahead of print 1 July 2019. DOI: 10.1128/CMR.00135-18.

4. **Johnson JR, Russo TA**. Molecular Epidemiology of Extraintestinal Pathogenic Escherichia coli. *EcoSal Plus*;8. Epub ahead of print 8 February 2018. DOI: 10.1128/ecosalplus.esp-0004-2017.

5. **Sarowska J, Futoma-Koloch B, Jama-Kmiecik A, Frej-Madrzak M, Ksiazczyk M, *et al.*** Virulence factors, prevalence and potential transmission of extraintestinal pathogenic Escherichia coli isolated from different sources: Recent reports. *Gut Pathogens* 2019;11:10.

6. **McNally A, Kallonen T, Connor C, Abudahab K, Aanensen DM, *et al.*** Diversification of colonization factors in a multidrug-resistant escherichia coli lineage evolving under negative frequency- dependent selection. *MBio*;10. Epub ahead of print 1 March 2019. DOI: 10.1128/mBio.00644-19.

7. **Chattaway MA, Aboderin AO, Fashae K, Okoro CK, Opintan JA, *et al.*** Fluoroquinolone-resistant enteric bacteria in sub-saharan Africa: Clones, implications and research needs. *Frontiers in Microbiology* 2016;7:558.

8. **Alonso CA, Zarazaga M, Ben Sallem R, Jouini A, Ben Slama K, *et al.*** Antibiotic resistance in Escherichia coli in husbandry animals: the African perspective. *Letters in Applied Microbiology* 2017;64:318–334.

9. **Khairy RM, Mohamed ES, Abdel Ghany HM, Abdelrahim SS**. Phylogenic classification and virulence genes profiles of uropathogenic E. coli and diarrhegenic E. coli strains isolated from community acquired infections. *PLoS One* 2019;14:e0222441.

10. **Forson AO, Tsidi WB, Nana-Adjei D, Quarchie MN, Obeng-Nkuramah N**. Escherichia coli bacteriuria in pregnant women in Ghana: Antibiotic resistance patterns and virulence factors. *BMC Res Notes* 2018;11:901.

11. **Huynh BT, Padget M, Garin B, Herindrainy P, Kermorvant-Duchemin E, *et al.*** Burden of bacterial resistance among neonatal infections in low income countries: How convincing is the epidemiological evidence? *BMC Infect Dis* 2015;15:127.

12. **Seni J, Peirano G, Okon KO, Jibrin YB, Mohammed A, *et al.*** The population structure

of clinical extra-intestinal Escherichia coli in a teaching hospital from Nigeria. *Diagn Microbiol Infect Dis* 2018;92:46–49.

13. **Okonko IO, Donbraye-Emmanuel OB, Ijandipe LA, Ogun AA, Adedeji AO, *et al.*** Antibiotics Sensitivity and Resistance Patterns of Uropathogens to Nitrofurantoin and Nalidixic Acid in Pregnant Women with Urinary Tract Infections in Ibadan, Nigeria. *Middle-East J Sci Res* 2009;4:105–109.

14. **Ogbolu DO, Piddock LJV, Webber MA**. Opening Pandora's box: High-level resistance to antibiotics of last resort in Gram-negative bacteria from Nigeria. *J Glob Antimicrob Resist* 2020;21:211–217.

15. **Duru C, Olanipekun G, Odili V, Kocmich N, Rezac A, *et al.*** Molecular characterization of invasive Enterobacteriaceae from pediatric patients in Central and Northwestern Nigeria. *PLoS One* 2020;15:e0230037.

16. **Sands K, Carvalho MJ, Portal E, Thomson K, Dyer C, *et al.*** Characterization of antimicrobial-resistant Gram-negative bacteria that cause neonatal sepsis in seven low- and middle-income countries. *Nat Microbiol 2021 64* 2021;6:512–523.

17. **CLSI**. M100 Performance Standards for Antimicrobial Susceptibility Testing A CLSI supplement for global application. Performance Standards for Antimicrobial Susceptibility Testing Performance Standards for Antimicrobial Susceptibility Testing. https://www.academia.edu/41587236/M100_Performance_Standards_for_Antimicrobial_Susceptibility_Testing_A_CLSI_supplement_for_global_application_28th_Edition (2020, accessed 6 August 2020).

18. **Berends MS, Luz CF, Friedrich AW, Sinha BNM, Albers CJ, *et al.*** AMR - An R package for working with antimicrobial resistance data. *bioRxiv* 2019;810622.

19. **Wakimoto N, Nishi J, Sheikh J, Nataro JP, Sarantuya J, *et al.*** Quantitative biofilm assay using a microtiter plate to screen for enteroaggregative Escherichia coli. *Am J Trop Med Hyg* 2004;71:687–690.

20. **Naves P, Prado G Del, Huelves L, Gracia M, Ruiz V, *et al.*** Measurement of biofilm formation by clinical isolates of Escherichia coli is method-dependent. *J Appl Microbiol* 2008;105:585–590.

21. **Afolayan AO, Oaikhena AO, Aboderin AO, Olabisi OF, Amupitan AA, *et al.*** Clones and Clusters of Antimicrobial-Resistant Klebsiella from Southwestern Nigeria. *bioRxiv* 2021;2021.06.21.449255.

22. **Underwood A**. GHRU (Genomic Surveillance of Antimicrobial Resistance) Retrospective 1 Bioinformatics Methods. https://www.protocols.io/view/ghru-genomic-surveillance-of-antimicrobial-resista-bpn6mmhe (2020, accessed 9 January 2022).

23. **Croucher NJ, Page AJ, Connor TR, Delaney AJ, Keane JA, *et al.*** Rapid phylogenetic analysis of large samples of recombinant bacterial whole genome sequences using Gubbins. *Nucleic Acids Res* 2015;43:e15.

24. **Argimón S, Abudahab K, Goater RJE, Fedosejev A, Bhai J, *et al.*** Microreact: visualizing and sharing data for genomic epidemiology and phylogeography. *Microb genomics* 2016;2:e000093.

25. **Letunic I, Bork P**. Interactive Tree Of Life (iTOL) v5: an online tool for phylogenetic tree display and annotation. *Nucleic Acids Res* 2021;49:W293–W296.

26. **Inouye M, Dashnow H, Raven LA, Schultz MB, Pope BJ, *et al.*** SRST2: Rapid genomic surveillance for public health and hospital microbiology labs. *Genome Med* 2014;6:006627.

27. **Ingle DJ, Levine MM, Kotloff KL, Holt KE, Robins-Browne RM**. Dynamics of antimicrobial resistance in intestinal Escherichia coli from children in community settings in South Asia and sub-Saharan Africa. *Nat Microbiol* 2018;3:1063–1073.

28. **Conway JR, Lex A, Gehlenborg N**. UpSetR: An R package for the visualization of intersecting sets and their properties. *Bioinformatics* 2017;33:2938–2940.

29. **Hunt M, Mather AE, Sánchez-Busó L, Page AJ, Parkhill J, *et al.*** ARIBA: Rapid antimicrobial resistance genotyping directly from sequencing reads. *Microb Genomics*;3. Epub ahead of print 1 October 2017. DOI: 10.1099/mgen.0.000131.

30. **Chen L, Yang J, Yu J, Yao Z, Sun L, *et al.*** VFDB: a reference database for bacterial virulence factors. DOI: 10.1093/nar/gki008.

31. **Carattoli A, Zankari E, Garciá-Fernández A, Larsen MV, Lund O, *et al.*** In Silico

detection and typing of plasmids using plasmidfinder and plasmid multilocus sequence typing. *Antimicrob Agents Chemother* 2014;58:3895–3903.

32. **Wirth T, Falush D, Lan R, Colles F, Mensa P, *et al.*** Sex and virulence in Escherichia coli: An evolutionary perspective. *Mol Microbiol* 2006;60:1136–1151.

33. **Clausen PTLC, Aarestrup FM, Lund O**. Rapid and precise alignment of raw reads against redundant databases with KMA. *BMC Bioinformatics* 2018;19:1–8.

34. **Camacho C, Coulouris G, Avagyan V, Ma N, Papadopoulos J, *et al.*** BLAST+: Architecture and applications. *BMC Bioinformatics*;10. Epub ahead of print 15 December 2009. DOI: 10.1186/1471-2105-10-421.

35. **Beghain J, Bridier-Nahmias A, Nagard H Le, Denamur E, Clermont O**. ClermonTyping: An easy-to-use and accurate in silico method for Escherichia genus strain phylotyping. *Microb Genomics* 2018;4:e000192.

36. **Kahlmeter G, Giske CG, Kirn TJ, Sharp SE**. Point-counterpoint: Differences between the European Committee on Antimicrobial susceptibility testing and Clinical and Laboratory standards institute recommendations for reporting antimicrobial susceptibility results. *J Clin Microbiol*;57. Epub ahead of print 1 September 2019. DOI: 10.1128/JCM.01129-19.

37. **Schwengers O, Jelonek L, Dieckmann MA, Beyvers S, Blom J, *et al.*** Bakta: rapid and standardized annotation of bacterial genomes via alignment-free sequence identification. *Microb Genomics* 2021;7:000685.

38. **Rutherford K, Parkhill J, Crook J, Horsnell T, Rice P, *et al.*** Artemis: sequence visualization and annotation. *Bioinformatics* 2000;16:944–945.

39. **Carver TJ, Rutherford KM, Berriman M, Rajandream M-A, Barrell BG, *et al.*** ACT: the Artemis comparison tool. *Bioinformatics* 2005;21:3422–3423.

40. **Gilchrist CLM, Chooi Y-H**. clinker & clustermap.js: automatic generation of gene cluster comparison figures. *Bioinformatics* 2021;37:2473–2475.

41. **Arredondo-Alonso S, Rogers MRC, Braat JC, Verschuuren TD, Top J, *et al.*** mlplasmids: a user-friendly tool to predict plasmid- and chromosome-derived sequences

for single species. *Microb Genomics* 2018;4:e000224.

42. **Roer L, Hansen F, Frølund Thomsen MC, Knudsen JD, Hansen DS, *et al.*** WGS-based surveillance of third-generation cephalosporin-resistant Escherichia coli from bloodstream infections in Denmark. *J Antimicrob Chemother* 2017;72:1922–1929.

43. **Schürch AC, Arredondo-Alonso S, Willems RJL, Goering R V.** Whole genome sequencing options for bacterial strain typing and epidemiologic analysis based on single nucleotide polymorphism versus gene-by-gene–based approaches. *Clin Microbiol Infect* 2018;24:350–354.

44. **Ludden C, Coll F, Gouliouris T, Restif O, Blane B, *et al.*** Defining nosocomial transmission of Escherichia coli and antimicrobial resistance genes: a genomic surveillance study. *The Lancet Microbe* 2021;2:e472.

45. **Ideses D, Gophna U, Paitan Y, Chaudhuri RR, Pallen MJ, *et al.*** A degenerate type III secretion system from septicemic Escherichia coli contributes to pathogenesis. *J Bacteriol* 2005;187:8164–8171.

46. **Schaufler K, Semmler T, Wieler LH, Trott DJ, Pitout J, *et al.*** Genomic and functional analysis of emerging virulent and multidrug-resistant Escherichia coli lineage sequence type 648. *Antimicrob Agents Chemother*;63. Epub ahead of print 1 June 2019. DOI: 10.1128/AAC.00243-19.

47. **Fang CT, Chuang YP, Shun CT, Chang SC, Wang JT**. A Novel Virulence Gene in Klebsiella pneumoniae Strains Causing Primary Liver Abscess and Septic Metastatic Complications. *J Exp Med* 2004;199:697–705.

48. **Touzé T, Tran AX, Hankins J V, Mengin-Lecreulx D, Trent MS**. Periplasmic phosphorylation of lipid A is linked to the synthesis of undecaprenyl phosphate. *Mol Microbiol* 2008;67:264.

49. **Forde BM, Zowawi HM, Harris PNA, Roberts L, Ibrahim E, *et al.*** Discovery of mcr-1 -Mediated Colistin Resistance in a Highly Virulent Escherichia coli Lineage . *mSphere*;3. Epub ahead of print 31 October 2018. DOI: 10.1128/MSPHERE.00486-18.

50. **Hagiya H, Watanabe N, Maki M, Murase T, Otsuka F**. Clinical utility of string test as a screening method for hypermucoviscosity-phenotype K lebsiella pneumoniae. *Acute*

Med Surg 2014;1:245–246.

51. **Magiorakos AP, Srinivasan A, Carey RB, Carmeli Y, Falagas ME, *et al.*** Multidrug-resistant, extensively drug-resistant and pandrug-resistant bacteria: An international expert proposal for interim standard definitions for acquired resistance. *Clin Microbiol Infect* 2012;18:268–281.

52. **Aboderin OA, Abdu LR, Odetoyin BW, Lamikanra A**. Antimicrobial resistance in Escherichia coli strains from urinary tract infections. *J Natl Med Assoc* 2009;101:1268–1273.

53. **Onanuga A, Mahindroo J, Singh S, Taneja N**. Phenotypic and molecular characterization of antimicrobial resistant escherichia coli from urinary tract infections in port-harcourt, nigeria. *Pan Afr Med J*;34. Epub ahead of print 2019. DOI: 10.11604/pamj.2019.34.144.18182.

54. **Tegha G, Ciccone EJ, Krysiak R, Kaphatika J, Chikaonda T, *et al.*** Genomic epidemiology of Escherichia coli isolates from a tertiary referral center in Lilongwe, Malawi. *Microb Genomics* 2020;7:000490.

55. **Lim C, Takahashi E, Hongsuwan M, Wuthiekanun V, Thamlikitkul V, *et al.*** Epidemiology and burden of multidrug-resistant bacterial infection in a developing country. *Elife*;5. Epub ahead of print 6 September 2016. DOI: 10.7554/eLife.18082.

56. **Russo TA, Wenderoth S, Carlino UB, Merrick JM, Lesse AJ**. Identification, genomic organization, and analysis of the group III capsular polysaccharide genes kpsD, kpsM, kpsT, and kpsE from an extraintestinal isolate of Escherichia coli (CP9, O4/K54/H5). *J Bacteriol* 1998;180:338–349.

57. **Lamikanra A, Crowe JL, Lijek RS, Odetoyin BW, Wain J, *et al.*** Rapid evolution of fluoroquinolone-resistant Escherichia coli in Nigeria is temporally associated with fluoroquinolone use. *BMC Infect Dis*;11. Epub ahead of print 7 November 2011. DOI: 10.1186/1471-2334-11-312.

58. **Musicha P, Cornick JE, Bar-Zeev N, French N, Masesa C, *et al.*** Trends in antimicrobial resistance in bloodstream infection isolates at a large urban hospital in Malawi (1998–2016): a surveillance study. *Lancet Infect Dis* 2017;17:1042–1052.

59. **Rawat D, Nair D**. Extended-spectrum ß-lactamases in gram negative bacteria. *J Glob Infect Dis* 2010;2:263.

60. **Mitchell SL, Simner PJ**. Next-Generation Sequencing in Clinical Microbiology: Are We There Yet? *Clinics in Laboratory Medicine* 2019;39:405–418.

61. **Rossen JWA, Friedrich AW, Moran-Gilad J**. Practical issues in implementing whole-genome-sequencing in routine diagnostic microbiology. *Clinical Microbiology and Infection* 2018;24:355–360.

62. **Borges CA, Tarlton NJ, Riley LW**. Escherichia coli from Commercial Broiler and Backyard Chickens Share Sequence Types, Antimicrobial Resistance Profiles, and Resistance Genes with Human Extraintestinal Pathogenic Escherichia coli. *Foodborne Pathog Dis* 2019;16:813–822.

63. **Gauthier L, Dortet L, Cotellon G, Creton E, Cuzon G, *et al.*** Diversity of carbapenemase-producing Escherichia coli isolates in France in 2012-2013. *Antimicrobial Agents and Chemotherapy*;62. Epub ahead of print 1 August 2018. DOI: 10.1128/AAC.00266-18.

64. **Sartori L, Fernandes MR, Ienne S, de Souza TA, Gregory L, *et al.*** Draft genome sequences of two fluoroquinolone-resistant CTX-M-15-producing Escherichia coli ST90 (ST23 complex) isolated from a calf and a dairy cow in South America. *Journal of Global Antimicrobial Resistance* 2017;11:145–147.

Figures and Tables

Table 1: Distribution of Sequence Types (ST) and Resistance Profiles (RP) within Sentinel Sites

Sentinel Site	No. of Isolates	No. of Observed STs	Most Prevalent ST (number)	No. of Observed Resistance Profile	Most Prevalent Resistance Profile (total number, STs (number))
OAU	18	10	ST131 (6)	9	RP-1: AMP CIP CRO CXM CXMA GEN NAL SXT (n = 5; ST131 (n = 3))
UCH	22	15	ST131 (5)	14	RP-5: AMP SXT (n = 4, ST12 (n = 2), ST942 (n = 2))
LAU	28	18	ST156 (4) & ST90 (4)	14	RP-2: AMP CIP CXMA GEN NAL SXT (Total = 7, ST156 (n = 3), ST90 (n = 3))

A

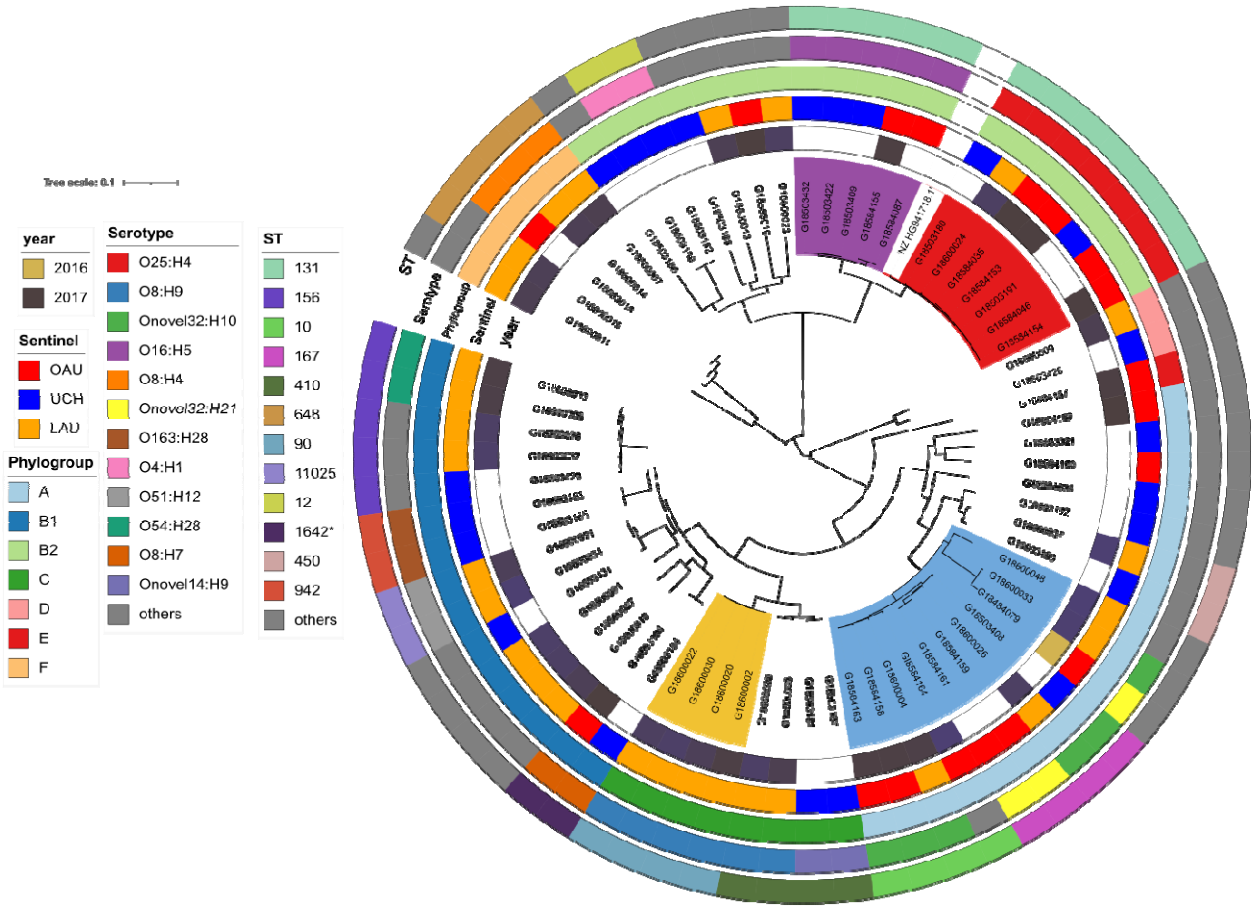

Figure 1: Maximum likelihood SNP tree of bloodstream *E. coli* isolates sequenced for this study. The purple-coloured clade represent ST131 lineage 1 (O16:H5 serotype); the red clade represent the ST131 lineage 2 (O25:H4 serotype) ; the blue clade represent the ST10-ST167 clade ; The light brown clade mark the cluster from a single site representing likely outbreak clone of ST90 (b) The ST90 likely outbreak cluster of O8:H9 strains, showing resistance and plasmid profiles

A.

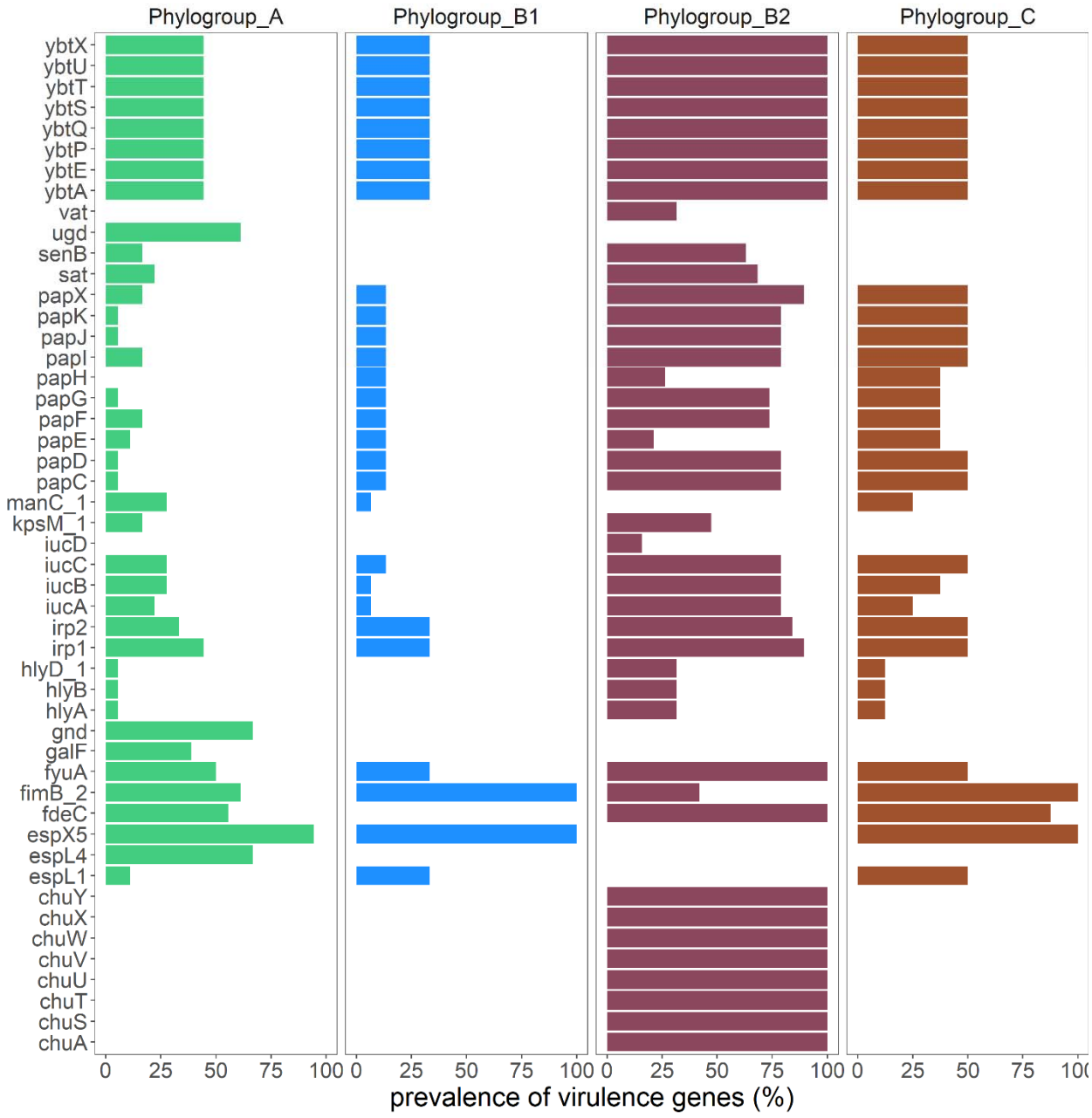
Phylogroup_A
Phylogroup_B1
Phylogroup_B2
Phylogroup_C
ybtX
ybtU
ybtT
ybtS
ybtQ
ybtP
ybtE
ybtA
vat
ugd
senB
sat
papX
papK
papJ
papI
papH
papG
papF
papE
papD
papC
manC_1
kpsM_1
iucD
iucC
iucB
iucA
irp2
irp1
hlyD_1
hlyB
hlyA
gnd
galF
fyuA
fimB_2
fdeC
espX5
espL4
espL1
chuY
chuX
chuW
chuV
chuU
chuT
chuS
chuA
0 25 50 75 100
prevalence of virulence genes (%)

B

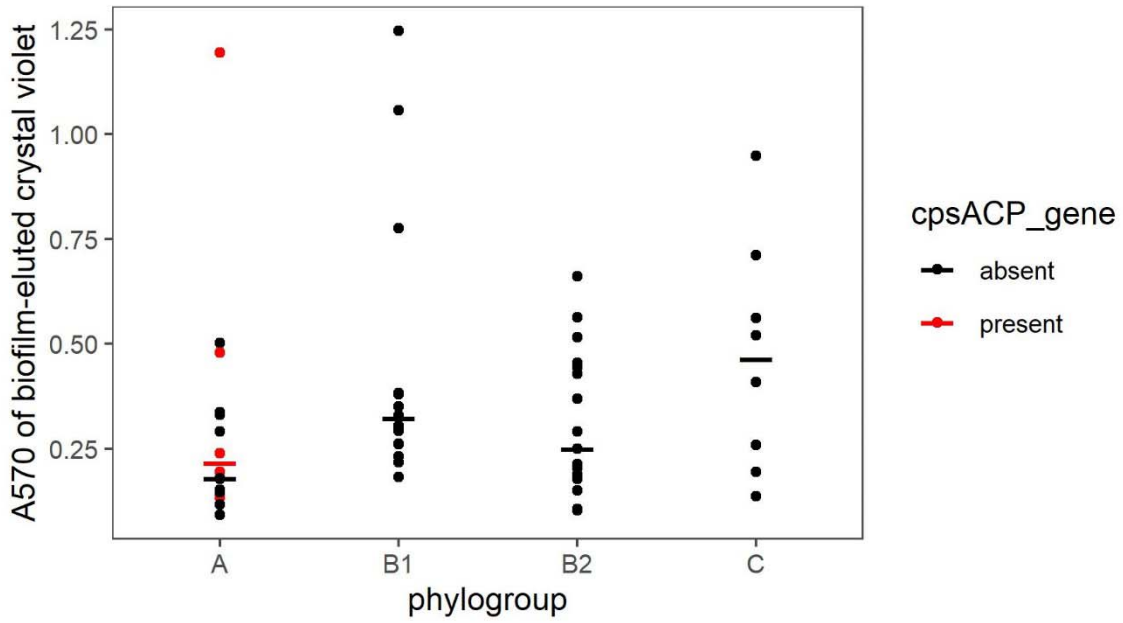

Fig. 2: a. Comparison of virulence genes among isolates clustered within phylogroups A-C. Graph shows the prevalence of virulence factors in isolates within phylogroups containing more than five isolates: A (n = 18), phylogroup B1 (n = 15), phylogroup B2 (n = 19), and phylogroup C (n = 8). Using Fisher's test ($p < 0.05$), only the VAGs significantly more prevalent in at least one phylogroup are shown. B. Biofilm formation in 67 strains, measured as A570 nm of crystal violet eluted from fixed and stained six-hour biofilms. Each dot represents data from a single strain belonging to the phylogroup listed on the X axis. Horizontal bars mark the median for each phylogroup, outliers inclusive due to the small number of tested strains in each phylogroup. The A570 nm values for isolates carrying the cpsACP gene were represented as red dots.

A

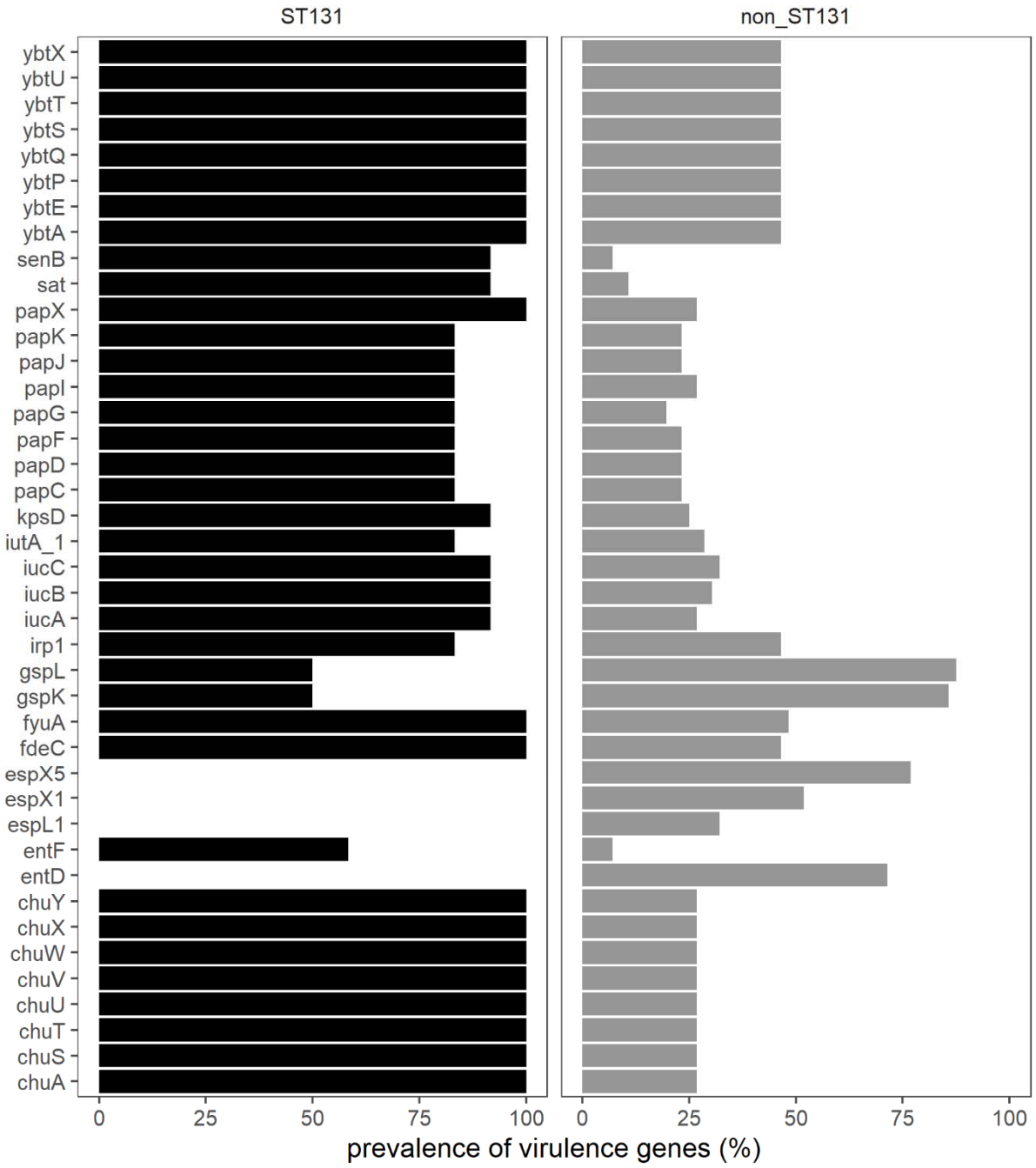
ST131
non_ST131
ybtX
ybtU
ybtT
ybtS
ybtQ
ybtP
ybtE
ybtA
senB
sat
papX
papK
papJ
papI
papG
papF
papD
papC
kpsD
iutA_1
iucC
iucB
iucA
irp1
gspL
gspK
fyuA
fdeC
espX5
espX1
espL1
entF
entD
chuY
chuX
chuW
chuV
chuU
chuT
chuS
chuA
0
25
50
75
100
prevalence of virulence genes (%)

B

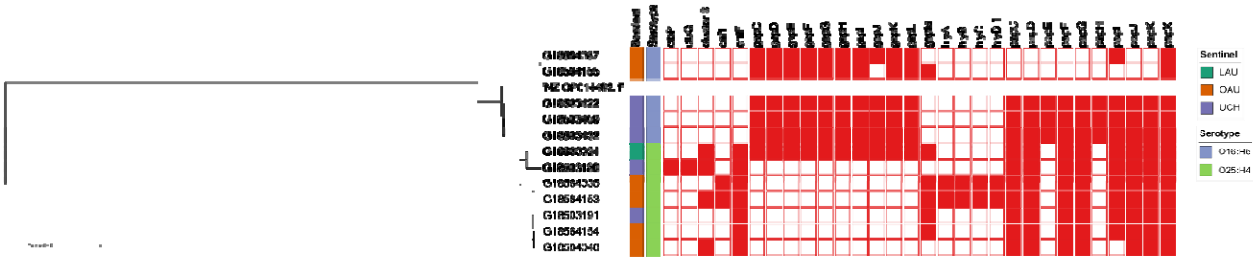

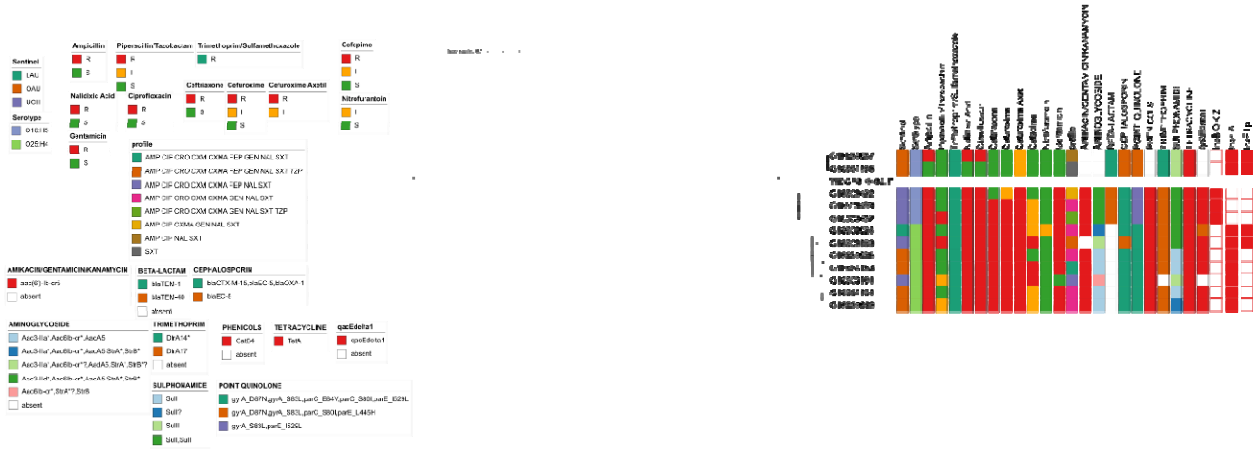

Fig. 3a: Comparison of virulence genes between ST131 (n = 12) and non-ST131 (n = 56) isolates. Using Fisher's test ($p < 0.05$, Bonferroni-corrected), only the VAGs significantly more prevalent in the STs are shown.

b: Virulence factor profile of isolates belonging to ST131. The presence or absence of a virulence gene is indicated by a red or white colour on the heatmap, respectively.

c. Antimicrobial resistance (AMR) phenotype profile and AMR genotype profile of isolates belonging to ST131. The presence or absence of plasmid Inc types is indicated by a red or white colour on the heatmap, respectively.

A

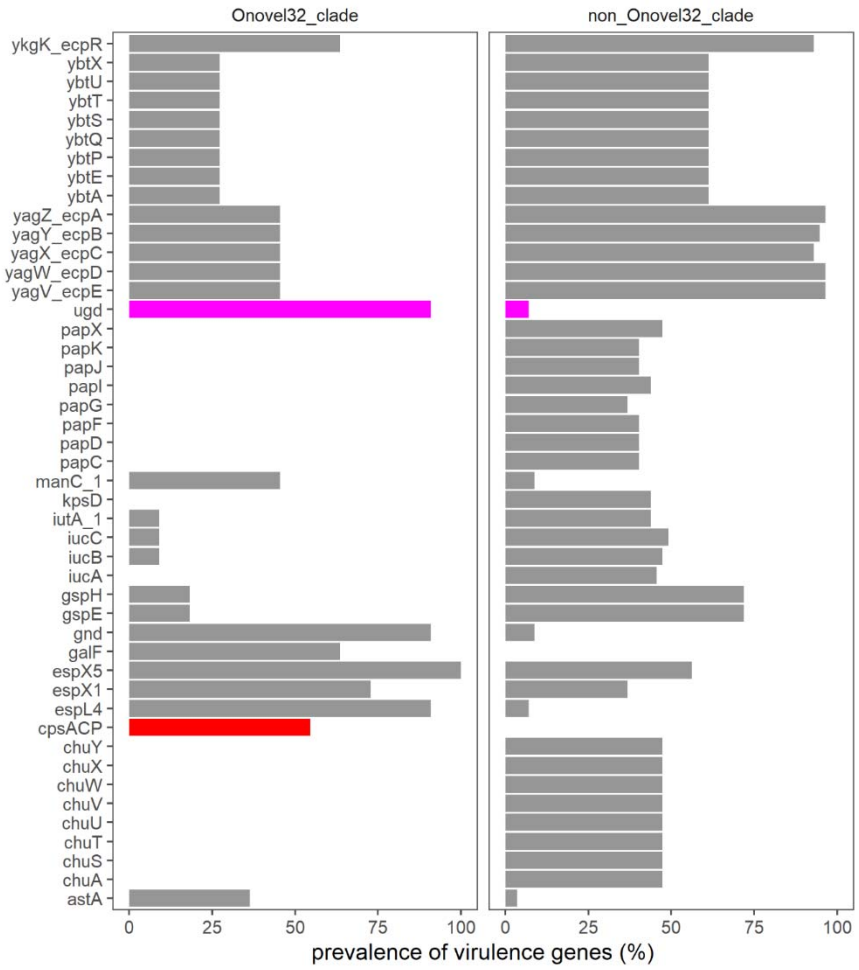
Onovel32_clade
non_Onovel32_clade
ykgK_ecpR
ybtX
ybtU
ybtT
ybtS
ybtQ
ybtP
ybtE
ybtA
yagZ_ecpA
yagY_ecpB
yagX_ecpC
yagW_ecpD
yagV_ecpE
ugd
papX
papK
papJ
papI
papG
papF
papD
papC
manC_1
kpsD
iutA_1
iucC
iucB
iucA
gspH
gspE
gnd
galF
espX5
espX1
espL4
cpsACP
chuY
chuX
chuW
chuV
chuU
chuT
chuS
chuA
astA
0
25
50
75
100
prevalence of virulence genes (%)

B

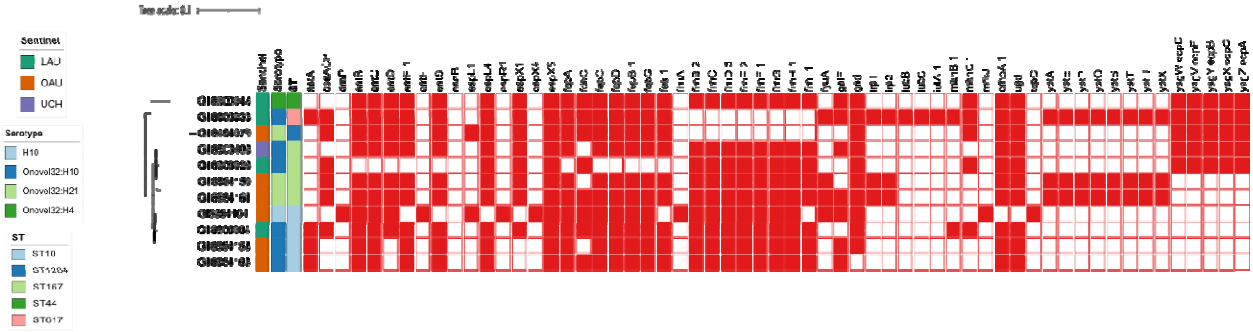
Sentinel
LAU
OAU
UCH
Serotype
H10
Onovel32:H10
Onovel32:H21
Onovel32:H4
ST
ST10
ST1284
ST167
ST44
ST617

Fig. 4a: Comparison of virulence genes between Onovel32 (n = 11) and non-Onovel32 (n = 57) clade isolates. Using Fisher's test ($p < 0.05$, Bonferroni-corrected), only the virulence genes significantly more prevalent are shown. The cpsACP gene and the ugd gene bars were coloured red and magenta, respectively.

b: Onovel32 clade isolates belonging to the sequence types ST10, ST167, and their locus variants belong to phylogroup A. Leaf tip colours differentiate the sentinel sites; OAU (Red), UCH (Blue), LAU (Yellow).

A

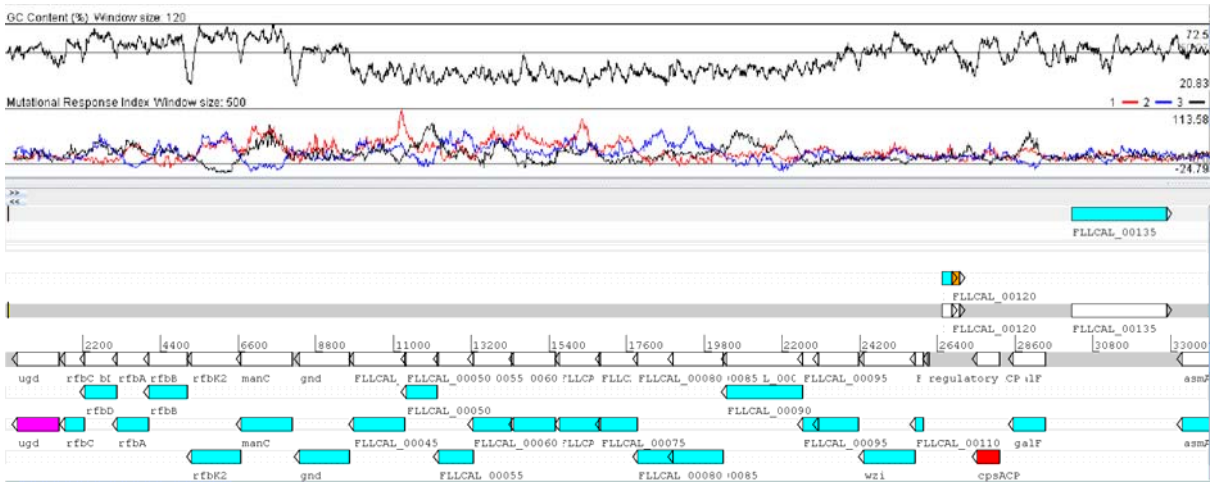

B

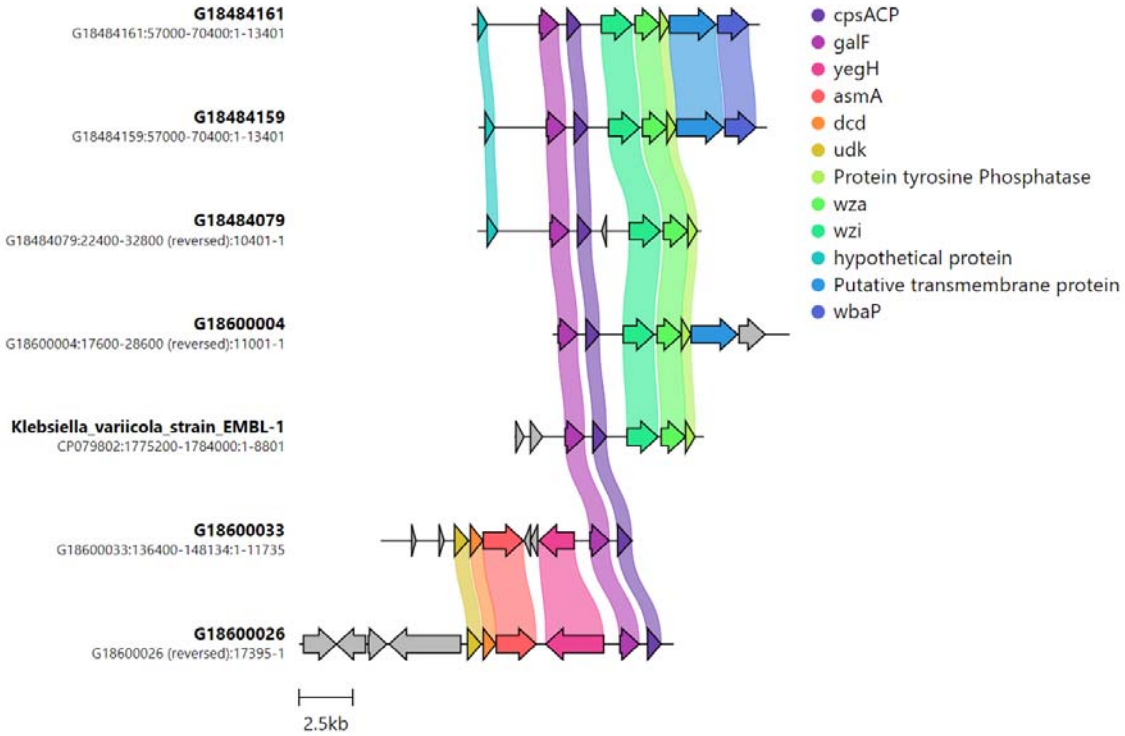

Figure 5a: Schematic cluster in ST1294 ONovel32 chromosome that includes the *ugd* and *cpsACP* genes. The genes within the cluster are syntenic and identical with a cluster from *Klebsiella variicola* (Accession number: CP079802.1). Above the schematic depiction of genes is a G+C content plot and mutational response index plot. (b) comparison of the ONovel32 cluster with analogous cluster in *Klebsiella variicola* strain EMBL-1

A

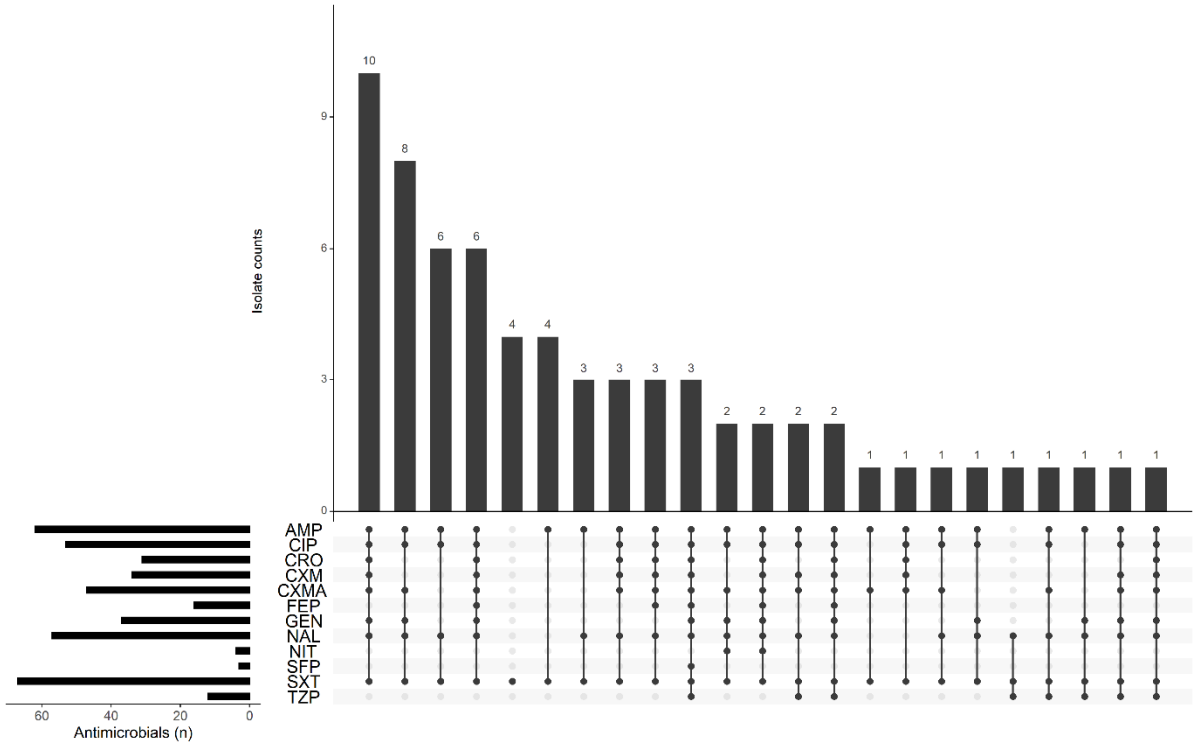

B

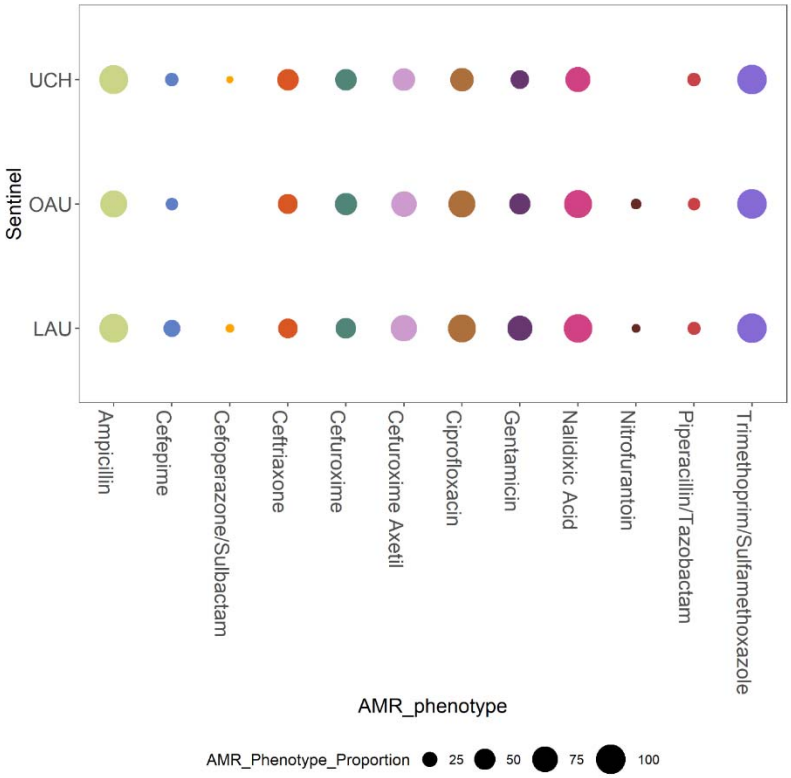

Fig. 6a: Resistance Profile of ExPEC isolates. The main bar chart demonstrates the number of ExPEC isolates with each combination of resistance to tested antibiotics, and is ordered in

descending order by the frequency of resistance profiles observed among 67 ExPEC isolates. The side bar chart demonstrates the number of isolates that are resistant to each of the named antibiotics. The dots and lines between dots at the base of the main bar chart (and the right side of the side bar chart) show the co-resistance status of the ExPEC isolates. All isolates were susceptible to Amikacin, Meropenem, Imipenem, and Ertapenem.

AMP = Ampicillin; CIP = Ciprofloxacin; CRO = Ceftriaxone; CXM = Cefuroxime; CXMA = Cefuroxime Axetil; FEP = Cefepime; GEN = Gentamicin; NAL = Nalidixic Acid; NIT = Nitrofurantoin; SFP = Cefoperazone/Sulbactam; SXT = Trimethoprim/Sulfamethoxazole; TZP = Piperacillin/Tazobactam

Fig. 6b: AMR phenotypes of ExPEC Isolates, stratified by Sentinel Site (LAU (n = 28), OAU (n = 22), UCH (n = 21)). The size of the coloured circles represent the proportion of isolates recovered from each sentinel site that demonstrated resistance to the tested antibiotics.

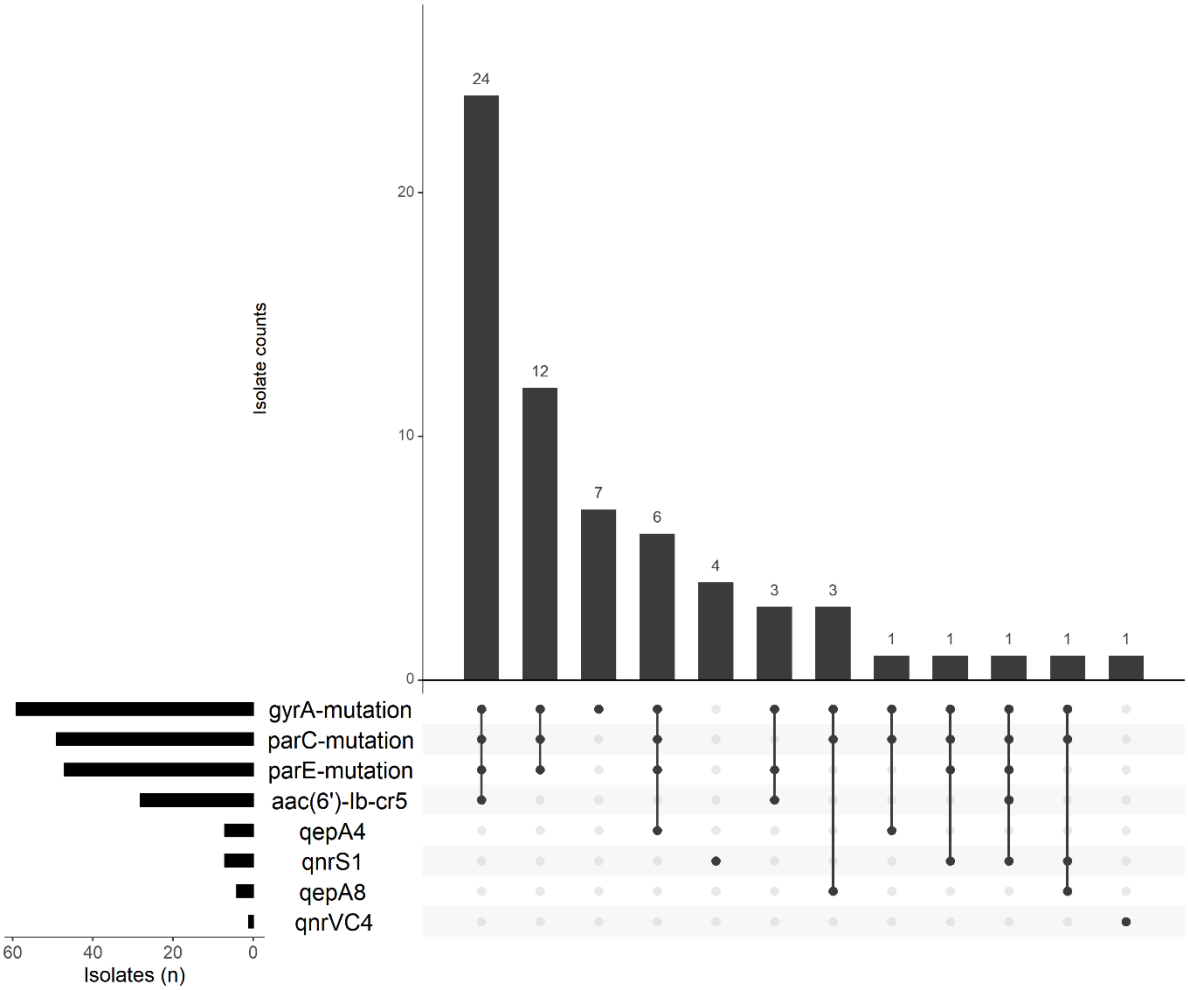
Isolate counts
24
12
7
6
4
3
3
1
1
1
1
1
0
10
20
gyrA-mutation
parC-mutation
parE-mutation
aac(6')-Ib-cr5
qepA4
qnrS1
qepA8
qnrVC4
60
40
20
0
Isolates (n)

843

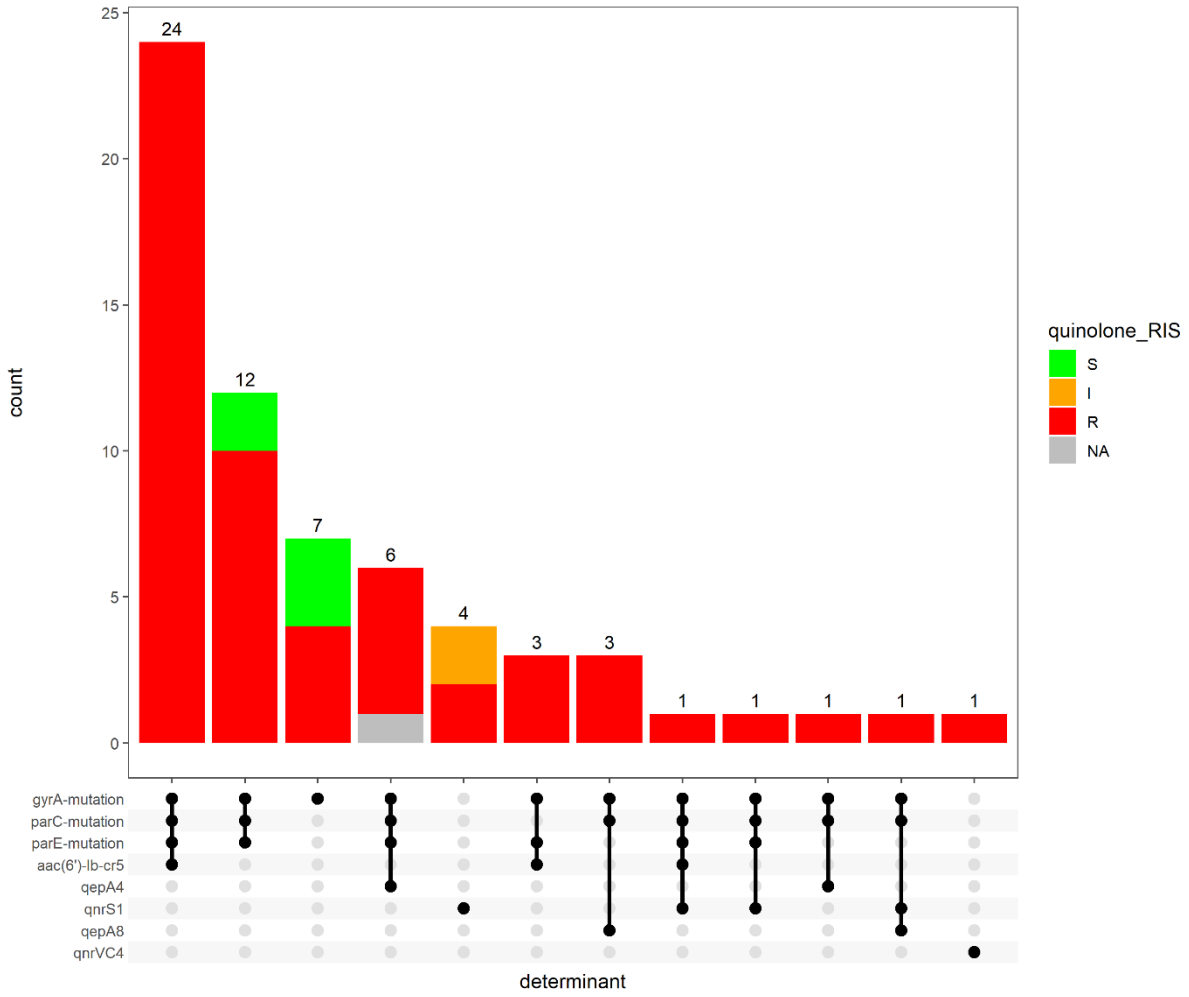

Fig. 7: Quinolone resistance gene combinations in ExPEC isolates. The upset plots show (a, b) the number of ExPEC isolates carrying each combination of genes conferring resistance to the quinolones (b), and is coloured by the proportion of observed phenotypic antimicrobial susceptibility, and is ordered in descending order by the frequency of resistance gene profiles observed. The side bar chart demonstrates the number of isolates that carry each of the resistance genes. The dots and lines between dots at the base of the main bar chart (and the right side of the side bar chart) show the co-resistance gene profile of the ExPEC isolates. From the legend of the coloured upset plot, NA means that phenotypic antimicrobial susceptibility data for the isolate is absent.

Supplementary Tables

Table S1: Resistance profiles of ExPEC isolates

Resistance Profile (number)	Resistance Profile code
AMP CIP CRO CXM CXMA GEN NAL SXT (10)	RP-1 (MDR)
AMP CIP CXMA GEN NAL SXT (8)	RP-2 (MDR)
AMP CIP CRO CXM CXMA FEP GEN NAL SXT (6)	RP-3 (MDR)
AMP CIP NAL SXT (6)	RP-4 (MDR)
AMP SXT (4)	RP-5
SXT (4)	RP-6
AMP CIP CRO CXM CXMA FEP GEN NAL SFP SXT TZP (3)	RP-7 (MDR)
AMP CIP CRO CXM CXMA FEP NAL SXT (3)	RP-8 (MDR)
AMP CIP CRO CXM CXMA NAL SXT (3)	RP-9 (MDR)
AMP NAL SXT (3)	RP-10 (MDR)
AMP CIP CRO CXM CXMA FEP GEN NAL NIT SXT (2)	RP-11 (MDR)
AMP CIP CRO CXM CXMA FEP GEN NAL SXT TZP (2)	RP-12 (MDR)
AMP CIP CXM CXMA NAL SXT TZP (2)	RP-13 (MDR)
AMP CIP CXMA GEN NAL NIT SXT (2)	RP-14 (MDR)
AMP CIP CRO CXM CXMA GEN NAL SXT TZP (1)	RP-other (MDR)
AMP CIP CRO CXM CXMA SXT (1)	RP-other (MDR)
AMP CIP CXM CXMA GEN NAL SXT TZP (1)	RP-other (MDR)
AMP CIP CXMA NAL SXT (1)	RP-other (MDR)
AMP CIP CXMA NAL SXT TZP (1)	RP-other (MDR)
AMP CIP GEN NAL SXT (1)	RP-other (MDR)
AMP CXMA SXT (1)	RP-other (MDR)
AMP GEN NAL SXT TZP (1)	RP-other (MDR)
NAL SXT TZP (1)	RP-other (MDR)

Table S2: Summary of Antibiotic Susceptibility Test data showing the number of *E. coli* isolates that were resistant to the named antibiotics.

Drug class	Drug	Resistance % (resistance (n)/species (n))
Aminoglycosides	Gentamicin (GEN)	55.20% (37/67)
Beta-lactams/penicillins	Ampicillin (AMP)	92.50% (62/67)
	Piperacillin/tazobactam (TZP)	17.90% (12/67)
Cephalosporins (2nd gen.)	Cefuroxime (CXM)	50.70% (34/67)
	Cefuroxime Axetil (CXMA)	70.10% (47/67)
Cephalosporins (3rd gen.)	Cefoperazone.Sulbactam (SFP)	4.50% (3/67)
	Ceftriaxone (CRO)	46.30% (31/67)
Cephalosporins (4th gen.)	Cefepime (FEP)	23.90% (16/67)
Other antibacterials	Nitrofurantoin (NIT)	6.00% (4/67)
Quinolones	Ciprofloxacin (CIP)	79.10% (53/67)
	Nalidixic acid (NAL)	85.10% (57/67)
Trimethoprims	Trimethoprim/sulfamethoxazole (SXT)	100.0% (67/67)

Table S3: Degree of Agreement between phenotypic antimicrobial susceptibility tests and genotypic predicted antimicrobial resistance

drug	Tests (N)	concordance (%)	TP	FP	TN	FN	specificity	Specificity lower limits	Specificity upper limits	sensitivity	Sensitivity lower limits	Sensitivity upper limits
Aminoglycosides	67	55.22	37	30	0	0	0	0	0.115703308	1	0.905109413	1
Beta-lactams	67	71.64	45	1	3	18	0.75	0.19412045	0.993690537	0.714285714	0.586538974	0.821070793
Cephalosporins	67	68.66	46	20	0	1	0	0	0.168433471	0.978723404	0.887062283	0.999461468
Quinolones	67	86.57	56	7	2	2	0.222222222	0.028144973	0.600093574	0.965517241	0.880922689	0.995796353
Trimethoprim	67	100	67	0	0	0	NA	0	1	1	0.946430346	1

(Table S3b). **Degree of Agreement between phenotypic antimicrobial susceptibility tests and genotypic predicted antimicrobial resistance in isolates belonging to the ST131, ST90, and ST10-167 clades.**

id	ST	Aminoglycosides AMR	Aminoglycosides AST	Betalactam AMR	Betalactam AST	Cephalosporins AMR	Cephalosporins AST	Quinolones AMR	Quinolones AST	Trimethoprim AMR	Trimethoprim AST
G18484079	1284	R	S	S	R	R	R	R	R	R	R
G18503180	131	R	R	S	R	R	R	R	R	R	R
G18503191	131	R	S	S	R	R	R	R	R	R	R
G18503409	131	R	R	R	R	R	R	R	R	R	R
G18503422	131	R	R	R	R	R	R	R	R	R	R
G18503432	131	R	R	R	R	R	R	R	R	R	R
G18584035	131	R	R	S	R	R	R	R	R	R	R
G18584046	131	R	R	S	R	R	R	R	R	R	R
G18584087	131	R	S	R	R	R	S	R	R	R	R
G18584153	131	R	R	S	R	R	R	R	R	R	R
G18584154	131	R	R	S	R	R	R	R	R	R	R
G18584155	131	R	S	R	S	R	S	R	S	R	R
G18584158	10	R	R	R	R	R	R	R	R	R	R
G18584159	167	R	R	R	R	R	R	R	R	R	R

G18584161	167	R	R	R	R	R	R	R	R	R	R
G18584163	10	R	R	R	R	R	R	R	R	R	R
G18600004	10	R	S	R	R	R	R	R	R	R	R
G18600024	131	R	R	S	R	R	R	R	R	R	R
G18600026	167	R	R	R	R	R	R	R	R	R	R
G18600033	617	R	R	S	R	R	R	R	R	R	R
G18600048	44	R	R	S	R	R	R	R	R	R	R
GI8584164	10	R	S	R	R	S	R	R	R	R	R
G18600002	90	R	R	R	R	R	R	R	R	R	R
G18600020	90	R	R	R	R	R	R	R	R	R	R
G18600022	90	R	R	R	R	R	R	R	R	R	R
G18600030	90	R	R	R	R	R	R	R	R	R	R

Table S3c: List of genes predicted to confer resistance to antibiotics belonging to the drug classes in Table S3a

Drug Classes	**AMR genes**
Aminoglycosides	aac(6')-Ie/aph(2")-Ia, aac(6')-Ib-cr5, catB8/aac(6')-Ib', aac(6')-30/aac(6')-Ib', aac(3)-IIe, aac(3)-IId, aac(6')-Ib4, ant(2")-Ia, aph(3')-Ia, aadA2, aph(3")-Ib, aph(6)-Id, aadA5, aadA13, aadA1, aadA8
Beta-lactams	blaTEM-1, blaOXA-2, blaTEM-90, blaTEM-57, blaTEM-40, blaTEM-84, blaZ, blaR1, blaTEM-135
Cephalosporins	blaCTX-M-15, blaEC-15, blaEC-5, blaOXA-1, blaEC-16, blaEC-18, blaCTX-M-27, blaEC-8, blaCMY-2, blaEC-19, blaCMY-42, blaTEM-187, blaVEB-1
Quinolones	gyrA, parC, and pare mutations, qepA4, qnrS1, qepA8, qnrVC4
Trimethoprim	dfrA12, dfrA17, dfrA7, dfrA14, dfrA29, dfrF, dfrB4, dfrA5, dfrA1

Table S4: Genotypic characteristics of the most common STs in the invasive microbial population.

ST (number of strains)	Phylo-group	Sentinel Site (number)	Serotype (number)	Most Prevalent Resistance Profile (number)	Most Prevalent AMR gene profile (number)	Most prevalent plasmid replicon profile (number)
ST131 (12)	B2	OAU (6) UCH (5) LAU (1)	O16:H5 (5), O25:H4 (7)	RP-1: AMP CIP CRO CXM CXMA GEN NAL SXT (5)	aac(6')-Ib-cr5; Aac3-IIa*,Aac6Ib-cr*,AadA5; blaCTX-M-15,blaEC-5,blaOXA-1; CatB4_602; DfrA17; gyrA_D87N,gyrA_S83L,parC_E84V,parC_S80I,parE_I529L; MphA_1663; qacEdelta1; SulI; TetA (n = 3) and	Col156; IncB_O_K_Z; IncFI; IncFIB_AP001918 (3) and
					aac(6')-Ib-cr5; Aac3-IId*,Aac6Ib-cr*,AadA5,StrA*,StrB*; blaCTX-M-15,blaEC-5,blaOXA-1; blaTEM-40; CatB4; DfrA17; gyrA_S83L,parE_I529L; MphA; qacEdelta1; SulII,SulI; TetA (3)	Col156; IncFI; IncFIA; IncFIB_AP001918 (3)
ST10 (4)	A	OAU (3) LAU (1)	Onovel32:H10 (3), H10 (1)	RP-14: AMP CIP CXMA GEN NAL NIT SXT (2)	Each isolate had a unique AMR gene profile	IncFI; IncFIA; IncFIB_AP001918; IncQ1 (2)
ST156 (5)	B1	LAU (4) UCH (1)	H45 (1), O174:H28 (1), O54:H28 (2),	RP-2: AMP CIP CXMA GEN NAL SXT (3)	Aac3-IId*,StrA*,StrB; blaEC-18; blaTEM-1; DfrA17; gyrA_D87N,gyrA_S83L,parC_S80I; qepA8; SulII*; TetB* (3)	IncFIA; IncFIB; IncQ1 (3)

			O76:H30 (1)			
ST167 (4)	A	OAU (2) LAU (1) UCH (1)	Onovel32:H10 (2), Onovel32:H21 (2)	Each isolate had a unique AST profile	Aac3-IId*; blaCTX-M-15,blaEC-15; blaTEM-1; gyrA_D87N,gyrA_S83L,parC_S80I,parE_S458A; TetB* (2)	IncFI; IncFIA; IncFIB_AP001918 (3)
ST410 (4)	C	LAU (2) UCH (2)	O8:H9 (2), Onovel14:H9 (2)	RP-9: AMP CIP CRO CXM CXMA NAL SXT (2)	Each isolate had a unique AMR gene profile	Col_MG828; IncFI; IncFIA; IncFIB_AP001918 (2)
ST648 (4)	F	LAU (3) OAU (1)	O153var1:H6 (1), O8:H4 (3)	RP-7: AMP CIP CRO CXM CXMA FEP GEN NAL SFP SXT TZP (2)	aac(6')-Ib-cr5; Aac3-IIa*,Aac6Ib-cr*,AadA5; blaCMY-42,blaCTX-M-15,blaEC-19,blaOXA-1; blaTEM-1; CatA1*,CatB4; DfrA17; gyrA_D87N,gyrA_S83L,parC_S80I,parE_S458A; MphA; qacEdelta1; SulI; TetB* (2).	Col_BS512; Col_BS512__1; IncFIA; IncFIB_AP001918; IncFII_p; IncI1 (2)
ST90 (4)	C	LAU (4)	O8:H9 (4)	RP-2: AMP CIP CXMA GEN NAL SXT (3)	aac3-IId, aac6Ib-cr, strA, strB; blaTEM-1; blaEC-16, blaOXA-1; gyrA_D87N, gyrA_S83L, parC_S80I, parE_S458A; dfrA17; mphA; sulII; tetB (4).	IncFI; IncFIA; IncFIB_AP001918; IncQ1 (4)

Table S5: Genotypic characteristics of Onovel32 genomes in the invasive microbial population.

id	Sentinel	ST	Serotype	Resistance gene profile	plasmid_profile
G18484079	OAU	1284	Onovel32:H21	AadA2*, StrA*?,StrB; blaCTX-M-15,blaEC-15; CatA2*; DfrA12; gyrA_D87N,gyrA_S83L,parC_S80I,parE_S458A; MphA; qacEdelta1; qepA4; SulII, SulI; TetB*	IncFI; IncFIA; IncFIB_AP001918; IncX1; IncX1_1
G18503408	UCH	167	Onovel32:H10	AadA2*,StrA*,StrB*; blaCTX-M-27, blaEC-15; CatA1*,CatA2*; DfrA12; gyrA_D87N,gyrA_S83L,parC_S80I,parE_S458A; MphA*?; qacEdelta1; qepA4; SulII, SulI; TetA,TetB*,TetM*	IncFI; IncFIA; IncFIB_AP001918; IncX2
G18584158	OAU	10	Onovel32:H10	aac(6')-Ib-cr5; Aac3-IId*,Aac6Ib-cr*,AadA5,StrA*,StrB; blaOXA-1; blaTEM-84; CatA1*,CatB4; DfrA17; gyrA_D87N,gyrA_S83L,parC_S80I,parE_S458A; MphA; qacEdelta1; SulII*; TetB*	IncFI; IncFIA; IncFIB_AP001918; IncQ1
G18584159	OAU	167	Onovel32:H21	Aac3-IId*; blaCTX-M-15, blaEC-15; blaTEM-1; gyrA_D87N,gyrA_S83L,parC_S80I,parE_S458A; TetB*	IncFI; IncFIA; IncFIB_AP001918
G18584161	OAU	167	Onovel32:H21	Aac3-IId*; blaCTX-M-15, blaEC-15; blaTEM-1; gyrA_D87N,gyrA_S83L,parC_S80I,parE_S458A; TetB*	IncFI; IncFIA; IncFIB_AP001918
G18584163	OAU	10	Onovel32:H10	aac(6')-Ib-cr5; Aac3-IId*,Aac6Ib-cr*,AadA5,StrA*,StrB; blaOXA-1; blaTEM-84; CatA1*,CatB4*; DfrA17; gyrA_D87N,gyrA_S83L,parC_S80I,parE_S458A;	IncFI; IncFIA; IncFIB_AP001918; IncQ1

				MphA; qacEdelta1; SulII*; TetB*	
G18600004	LAU	10	Onovel32:H10	AadA1*?,StrA*,StrB*; blaOXA-1; blaTEM-1; DfrA14; gyrA_D87N,gyrA_S83L,parC_S80I,parE_S458A; qepA4; SulII	IncFI; IncFIA; IncFIB_AP001918
G18600026	LAU	167	Onovel32:H10	Aac3-IId*; blaEC-15; blaTEM-1; CatA1*; DfrA12; gyrA_D87N,gyrA_S83L,parC_S80I,parE_S458A; MphA; qacEdelta1; qepA4; SulI; TetB*	IncFI; IncFIA; IncFIB_AP001918
G18600033	LAU	617	Onovel32:H10	aac(6')-Ib-cr5; Aac3-IIa*,Aac6Ib-cr*,AadA5,StrA*?,StrB; blaCTX-M-15,blaEC-15,blaOXA-1; CatB4; DfrA17; gyrA_D87N,gyrA_S83L,parC_S80I,parE_S458A; MphA; qacEdelta1; SulII, SulI; TetB*	IncFI; IncFIA; IncFIB_AP001918
G18600048	LAU	44	Onovel32:H4	aac(6')-Ib-cr5; Aac3-IIa*,Aac6Ib-cr*,AadA5; blaCTX-M-15,blaOXA-1; CatB4; DfrA17; gyrA_D87N,gyrA_S83L,parC_S80I,parE_S458T; qacEdelta1; SulI; TetB*	Col_MG828; IncFI; IncFIB_AP001918; IncX3
GI8584164	OAU	10	H10	AadA2*,StrA*,StrB,CatA1*; blaTEM-1; DfrA12; gyrA_D87N,gyrA_S83L,parC_S80I,parE_S458A; MphA,QepA2*; qacEdelta1; qepA4; SulII*,SulI; TetB*	ColRI; Col_BS512; IncP_6

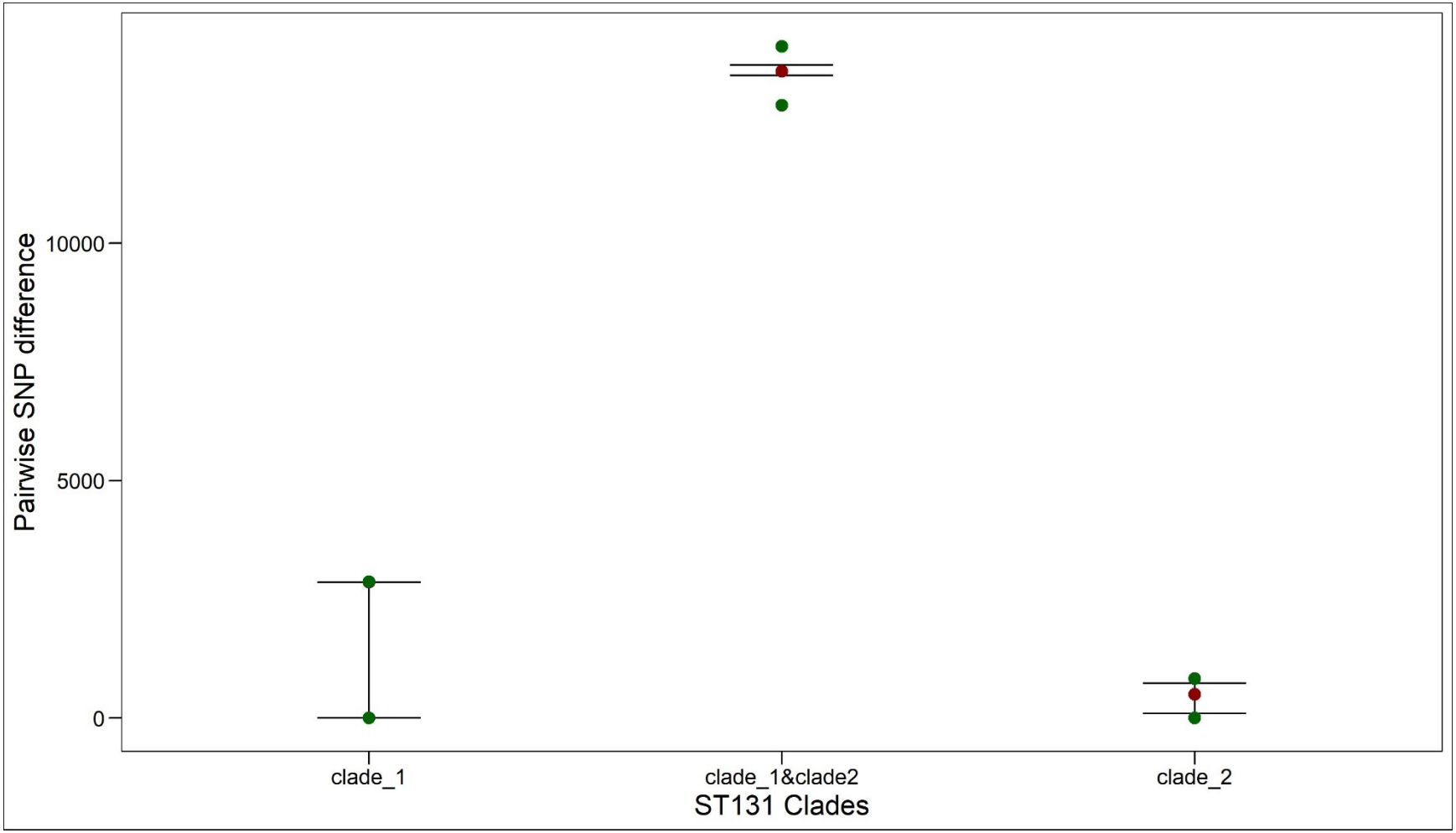

Supplementary Figure 1
Interclade (ST131 clade 1 and ST131 clade 2) distance between lineage ST131 isolates is greater than 10000 SNPs. The "whisker" plot shows the 25th percentile (lower point; green), median (red point), and the 75th percentile (upper point; green) of the pairwise SNP distances within and between lineages.

a)

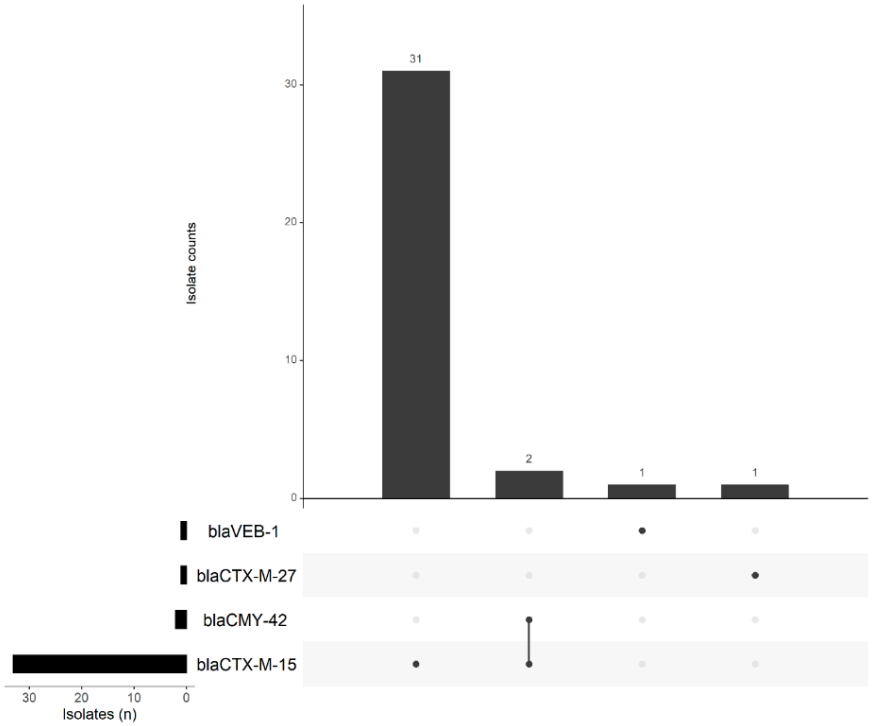

b.)

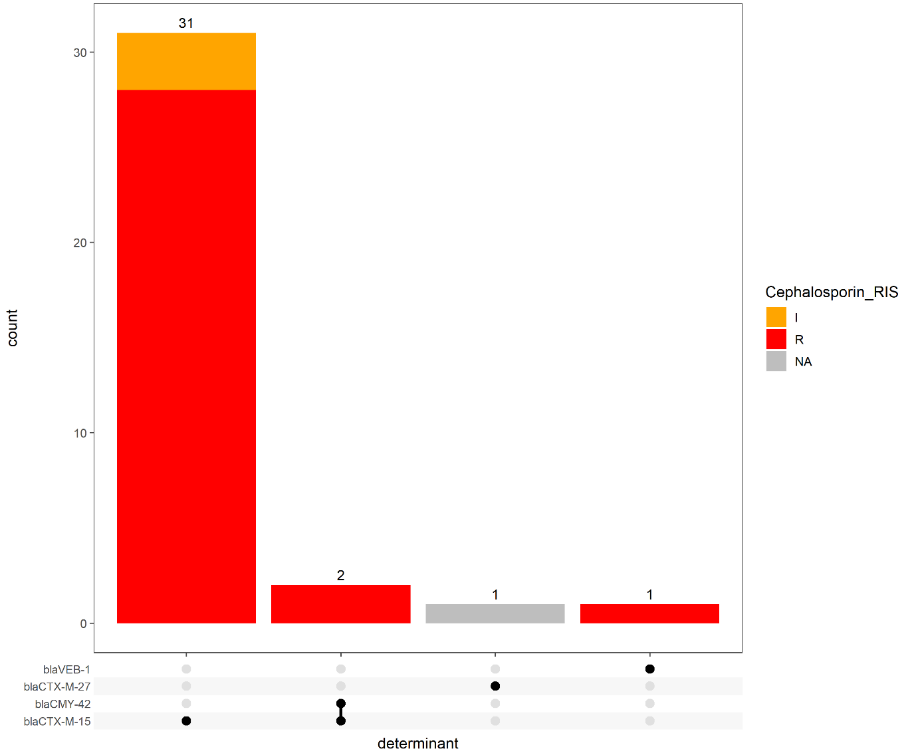

Supplementary Figure. 2: ESBL genes in ExPEC isolates. The upset plots demonstrate (a, b) the number of ExPEC isolates carrying each combination of genes conferring resistance to cephalosporins and (b), is coloured by the proportion of observed phenotypic antimicrobial susceptibility, and is ordered in descending order by the frequency of resistance gene profiles observed. The side bar chart (a) demonstrates the number of isolates that carry each of the resistance genes. The dots and lines between dots at the base of the main bar chart (and the right side of the side bar chart) show the co-resistance gene profile of the ExPEC isolates. From the legend of the coloured upset plot, NA means that there is no available data on phenotypic antimicrobial susceptibility data for the isolate.

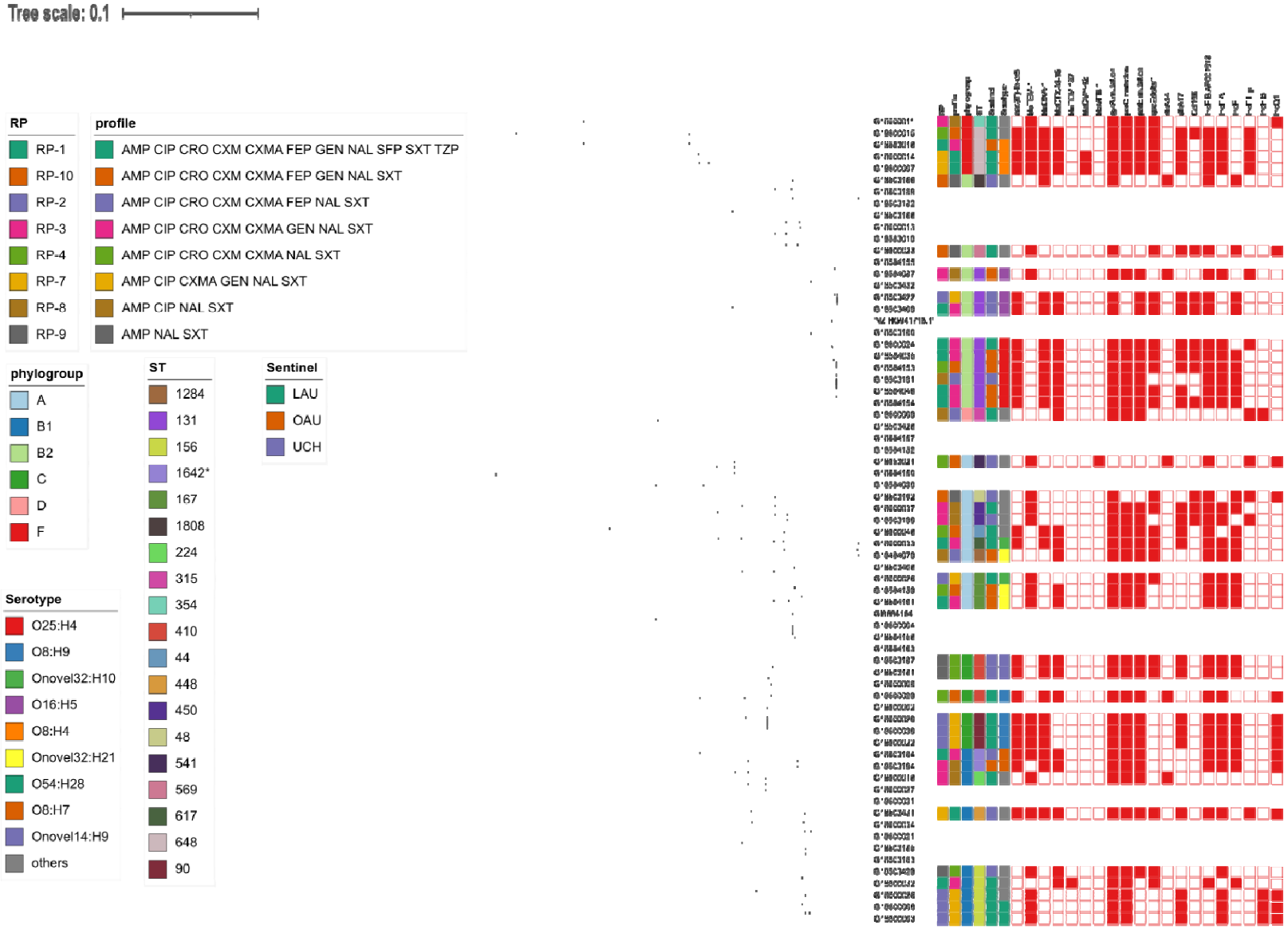

Supplementary Figure 3: Maximum likelihood SNP tree of bloodstream *E. coli* isolates sequenced for this study. Metadata for the 8 most common resistance profiles are shown in this figure. For the AMR genes and plasmid replicons, red colour indicates presence of the gene.